

PŘÍRODOVĚDECKÁ FAKULTA UNIVERZITY PALACKÉHO V OLMOUCI

KATEDRA OPTIKY



Příprava silně neklasických stavů světla a atomů

DIPLOMOVÁ PRÁCE

Karel Lemr

vedoucí diplomové práce:

doc. Mgr. Jaromír Fiurášek, Ph.D.

Olomouc

duben 2008

FACULTY OF SCIENCE, PALACKÝ UNIVERSITY OLMOUC

DEPARTMENT OF OPTICS



Generation of highly non-classical states of light and atoms

DIPLOMA THESIS

Karel Lemr

supervisor:

doc. Mgr. Jaromír Fiurášek, Ph.D.

Olomouc

April 2008

Contents

| | | |
|----------|--|-----------|
| 1 | Introduction | 6 |
| 1.1 | Historical background | 6 |
| 1.2 | Quantum information processing | 7 |
| 1.3 | Quantum memory | 8 |
| 1.4 | Goals of the present thesis | 9 |
| 2 | Methods and tools | 10 |
| 2.1 | Quantization of electromagnetic field | 10 |
| 2.2 | Quantum description of optical components | 12 |
| 2.2.1 | Beam splitter | 12 |
| 2.2.2 | Phase shifter | 14 |
| 2.2.3 | Polarizing beam splitter | 15 |
| 2.2.4 | Half-wave plate | 16 |
| 2.2.5 | Light squeezing | 16 |
| 2.3 | Quantum non-demolition interaction | 18 |
| 2.4 | Detection of light | 20 |
| 2.4.1 | Single photon detection | 20 |
| 2.4.2 | Homodyne detection | 21 |
| 2.5 | Numerical simulations | 22 |
| 3 | Preparation of two-photon entangled states in several spatial modes | 23 |
| 3.1 | Introduction | 23 |
| 3.2 | Motivation | 24 |

| | | |
|----------|--|-----------|
| 3.3 | Preparation scheme | 26 |
| 3.3.1 | Initialization phase | 27 |
| 3.3.2 | Preparation phase | 27 |
| 3.4 | Numerical simulations | 32 |
| 3.5 | Generalization to an arbitrary number of modes | 34 |
| 3.6 | Preparation of two-photon KLM states | 36 |
| 3.7 | Conclusions | 37 |
| 4 | Preparation of entangled atomic Dicke states | 39 |
| 4.1 | Introduction | 39 |
| 4.2 | Atoms-light interaction | 40 |
| 4.3 | Combination with displacement operator | 41 |
| 4.4 | Multiple interaction model | 42 |
| 4.5 | Numerical simulations | 44 |
| 4.6 | Conclusions | 45 |
| 5 | Conclusions | 47 |
| | Abstrakt diplomové práce | 49 |
| | Résumé de la thèse | 51 |

Chapter 1

Introduction

1.1 Historical background

In 1901, German physicist Max Planck published an article in *Annalen der Physik*, where he formulated a revolutionary idea, that energy exchange between light and matter is not continuous, but discrete [1]. There is a minimum amount of exchangeable energy, the so-called energy quantum containing energy of

$$E = h\nu, \tag{1.1}$$

where ν stands for the frequency of light and h is a proportionality constant, called the Planck constant to honor its discoverer. One may say, that all quantum physics began with this article after which many others have followed and the completely new physical theory has been build. It was named upon one of its key features - the quantum physics.

Brilliant minds of the beginning of the 20th century including Albert Einstein, Paul Adrien Maurice Dirac, Niels Bohr, David Bohm, Werner Karl Heisenberg, Erwin Rudolf Josef Schrödinger and many others have discovered important laws and formulated important principles of this new physical theory [2]. Somewhat intriguing properties of quantum physics have led to many different interpretations of the theory. The most commonly accepted interpretation has been formulated in Copenhagen by scientists around Niels Bohr in the late 20's. One can notice that laws of classical physics can often be obtained using several approximations on their quantum counterparts. This fact suggests that quantum physics is a more fundamental theory that enriches preceding theories.

Laws of quantum mechanics have been employed to study the physics at a microscale, such as the behaviour and properties of single atoms, molecules, electrons, neutrons, etc. Predictions of quantum mechanics have been confirmed by numerous experiments. Apart from particles, one can also use quantum physics to study fields. Formulation of quantum theory of electromagnetic field has been initiated by Dirac. Nobel prize winner, Roy Jay Glauber, can be considered the founder of quantum optics. Experiments in quantum optics often necessitate a strong coherent beam provided by laser. The invention of laser is therefore a significant mark in the timeline of quantum optics and it has stimulated further development in this area. Theoretical proposal of laser has been formulated by Charles Hard Townes and Arthur Leonard Schawlow in 1957 [3]. Important improvements have been suggested by Nikolay Basov and Aleksandr Prokhorov. In 1960, Theodore H. Maiman constructed the first laser using ruby crystal. The well known He-Ne laser has been constructed later in 1960 by Ali Javan in Iran.

Light and electromagnetic waves in general can be used as a very fast and reliable information carrier. Research in classical optics and electronics has led to development of daily used communication devices such as mobile phones or optical fibers. Quantum optics has opened further possibilities of using laws of quantum theory in information processing and communication with the goal of improving classical physics based technologies and enriching them by completely new features.

1.2 Quantum information processing

Quantum information processing (QIP) has demonstrated an important development in recent years [4]. The significant advances in implementing various protocols for QIP can, in the future, lead to long-distance quantum communication [5] or creation of a quantum computer [6]. Among many experimentally tested physical platforms, optical implementations appear particularly promising. A crucial prerequisite for optical quantum information processing is the ability to generate and manipulate various highly non-classical and entangled states of light beams. Entangled states of light are necessary for instance for quantum teleportation [7, 8, 9, 10], quantum gates in quantum computing with linear optics [11, 12, 13, 14, 15, 16, 17], or quantum repeaters [18].

These wide potential applications motivate the effort aimed at developing and demonstrating preparation protocols for various interesting quantum states of light. Single and two-photon Fock states were conditionally prepared from two-mode squeezed vacuum by measuring the number of photons in the idler mode [19, 20, 21, 22]. Schrödinger cat-like states were generated by subtracting a single photon from pulsed or continuous squeezed beams [23, 24, 25, 26, 27]. Photon-added coherent states were produced experimentally using down-conversion seeded with a weak coherent signal and conditioning on detection of a photon in the idler mode [28]. Schemes for preparation of arbitrary single-mode states via repeated addition or subtraction of single photons have been suggested [29, 30]. A universal procedure for conditional preparation of arbitrary multimode states of light with linear optics, single photons, coherent states and single-photon detectors has been developed [31].

A lot of attention has been paid to creation of two-mode N-photon entangled states, the so-called NOON states, [32, 33, 34, 35, 36, 37, 38, 39]. It was shown theoretically and demonstrated experimentally that such states can be conditionally generated from input single-photon states by multiphoton interference in a properly tailored interferometer. In a similar way, projection onto arbitrary NOON-type state can be accomplished [40]. The N-photon entangled states can find applications not only in quantum information processing, but can be also used for ultra-precise measurements [41, 42, 43, 44, 45] or quantum lithography [46, 47, 48]. For advanced applications, multimode entangled states will be required. However, the technique used for preparation of arbitrary two-mode N-photon states [32] cannot be immediately extended to multimode case.

1.3 Quantum memory

Light is a very good quantum information carrier and it can also be used to perform information processing. Quantum information needs however not only to be processed and transmitted, but it requires also the storage facilities. Storage of quantum information can not be done using classical means, but requires a special - quantum - memory. A very promising medium for quantum memory are atoms [49, 50, 51, 52, 53]. They can be trapped in the electromagnetic field [52] for a reasonable time or held in a glass cell [49].

A very promising interaction between light and atoms is the coupling between light beam

and collective atomic spin or pseudospin [54, 55, 56]. This interaction is experimentally feasible using either suitable cavity [57] of just a single passage of light through the atomic sample [58]. Discussion and comparison of these two approaches has been published in [59]. There are several other proposals for quantum memory using one to one atom-photon interaction [60, 61]. Usage of electromagnetically induced transparency has also been proposed to perform quantum memory [62].

The basic function of every memory, including the quantum one, is the capability of writing an information into the memory and the capability to read it back, when requested [58, 63, 64]. Quantum memory has multiple applications in QIP. It is indispensable for construction of quantum repeaters [65, 66], where it permits the entanglement swapping and distribution. Also quantum teleportation using atoms has been demonstrated [67]. Quantum memory can be used as a mediator to prepare specific quantum states of light [57, 68, 69].

For the quantum atomic memory to be useful, one needs to be able to prepare the atoms in desired quantum state. Several proposals have been made to obtain squeezed ground state of collective atomic spin [70] or the so-called Schrödinger cat states [71, 72, 73]. Entanglement between light beam and atoms [74] or a group of atoms [75] has also been proposed.

The key issue of all quantum memories using atoms is the decoherence that causes the information to be lost. Several studies have been performed to propose a long-lived quantum memory [76, 77].

1.4 Goals of the present thesis

One of the prerequisites for efficient QIP is the capability of preparation of various quantum states of light and atoms. In the present thesis, we propose two protocols for preparation of quantum states. Third chapter discusses preparation of two-photon states in several spatial modes. Proposal for preparation of atomic Dicke states is treated in the fourth chapter of this thesis. Both protocols are capable of preparation of highly non-classical quantum states with the prospect of their further applications in QIP.

Chapter 2

Methods and tools

2.1 Quantization of electromagnetic field

In classical theory of electromagnetic field, the energy density of free field in vacuum is in the form of

$$H = \frac{1}{2} \left(\epsilon_0 |\vec{E}|^2 + \mu_0 |\vec{H}|^2 \right), \quad (2.1)$$

where \vec{E} stands for the vector of intensity of electric field and \vec{H} stands for the vector of intensity of magnetic field, ϵ_0 is vacuum permittivity constant and μ_0 is vacuum permeability constant [4, 6, 78, 79, 80, 81]. In classical physics, one is able to obtain equations of motion from the energy expression such as (2.1) using the so-called Hamilton's principle. These equations of motion for vectors \vec{E} and \vec{H} manifest formal similarity with equations of motion of an infinite set of uncoupled linear harmonic oscillators, where every oscillator corresponds to one mode of the field. This similarity can be further exploited to construct quantum theory of light. In classical mechanics, overall energy of an infinite set of uncoupled one-dimensional linear harmonic oscillators with unit mass takes the form of

$$H = \sum_j \frac{1}{2} (P_j^2 + \omega_j^2 X_j^2), \quad (2.2)$$

where X_j and P_j are position and momentum of the j^{th} oscillator. It is straightforward to obtain the Hamilton operator of these oscillators just by replacing classical variables by quantum operators

$$\hat{H} = \frac{1}{2} (\hat{P}_j^2 + \omega_j^2 \hat{X}_j^2), \quad (2.3)$$

where \hat{X}_j and \hat{P}_j denote operators of position and momentum. Formal resemblance between the set of oscillators and the field leads us to conclusion that each mode of the field can be treated as quantized linear harmonic oscillator described by quadrature operators \hat{X}_j and \hat{P}_j . These operators are subsequently used for quantum description of light. Besides this approach, one can also build the whole quantum theory of light using canonical quantization which does not rely just on exploitation of formal similarity.

Quadrature operators \hat{X}_j and \hat{P}_j satisfy the well known canonical commutation relation

$$[\hat{X}_k, \hat{P}_j] = i\hbar\delta_{kj}, \quad (2.4)$$

that respects the fact that different modes are independent. For further calculations, it is convenient to rescale our quadrature operators

$$\hat{x}_k = \sqrt{\frac{\omega_k}{2\hbar}} \hat{X}_k, \quad \hat{p}_k = \frac{1}{\sqrt{2\hbar\omega_k}} \hat{P}_k \quad (2.5)$$

and recalculate commutation relations for new \hat{x}_k and \hat{p}_k

$$[\hat{x}_k, \hat{p}_j] = \frac{i}{2}\delta_{kj}. \quad (2.6)$$

In quantum mechanics of linear harmonic oscillators, it is convenient to define the creation \hat{a}_j^\dagger and annihilation \hat{a}_j operators

$$\begin{aligned} \hat{a}_j^\dagger &= \hat{x}_j - i\hat{p}_j, \\ \hat{a}_j &= \hat{x}_j + i\hat{p}_j, \end{aligned} \quad (2.7)$$

whose commutation relation reads

$$[\hat{a}_k, \hat{a}_j^\dagger] = \delta_{kj}. \quad (2.8)$$

The crucial role of these operators is in adding or subtracting one energy quantum each time they are applied. These operators have a similar meaning in quantization of light. They add or subtract one photon to/from the mode of light they are acting on. One can also express the Hamiltonian in terms of creation and annihilation operators

$$\hat{H}_j = \hbar\omega_k(\hat{a}_j^\dagger\hat{a}_j + \frac{1}{2}) = \hbar\omega_k(\hat{N}_j + \frac{1}{2}). \quad (2.9)$$

The operator $\hat{N}_k = \hat{a}_k^\dagger\hat{a}_k$ is called the photon number operator and it is the operator of the number of photons in the specified mode of light. Eigenstates of this operator are called Fock

states with eigenvalues denoting the number of photons in the specified mode

$$\hat{N}_j |n_j\rangle = n_j |n_j\rangle, \quad n_j = 0, 1, 2, \dots \quad (2.10)$$

Fock states form orthonormal basis and can be used to express other quantum states of light.

In Fock basis, one can also observe the action of creation and annihilation operators

$$\begin{aligned} \hat{a}_j^\dagger |n_j\rangle &= \sqrt{n_j + 1} |n_j + 1\rangle \\ \hat{a}_j |n_j\rangle &= \sqrt{n_j} |n_j - 1\rangle. \end{aligned} \quad (2.11)$$

Apart from \hat{N}_k , the Hamiltonian (2.9) contains also the second term ($\frac{1}{2}$). This term expresses the energy of vacuum that is omnipresent in each mode even if it contains no photons and it is also responsible for vacuum fluctuations.

2.2 Quantum description of optical components

The scheme for preparation of multimode two-photon states and the scheme for preparation of Dicke states of atomic ensemble discussed in the present thesis are composed of several elementary components, such as beam splitters, phase shifters, wave plates etc. These components perform transformations of one or several optical modes and a good quantum description of these devices is a necessary prerequisite for theoretical design and analysis of quantum state preparation schemes. In this section, we will briefly discuss their properties and quantum description.

2.2.1 Beam splitter

Beam splitter serves to mix two incident beams into two output beams. The situation is schematised in figure 2.1. Every beam splitter is described by one parameter - the amplitude transmittivity τ . In classical optics, this parameter describes, what portion of the amplitude of light in one incoming mode is transmitted through the beam splitter. The remaining portion of light ($\sqrt{1 - \tau^2}$) is reflected. It is convenient to define new parameter θ and set

$$\tau = \cos \theta, \quad \sqrt{1 - \tau^2} = \sin \theta. \quad (2.12)$$

In quantum theory of light, we replace light amplitude by annihilation operator \hat{a} . Let $\hat{a}_{j,\text{IN}}$, $j = 1, 2$ denotes the annihilation operator of the j^{th} input mode and $\hat{a}_{j,\text{OUT}}$, $j = 1, 2$

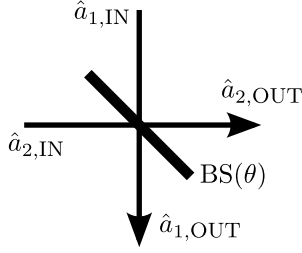


Figure 2.1: Beam splitter mixes two input modes into two output modes. In quantum theory of light, we describe incident and outgoing beams using annihilation operators. Beam splitter itself is then described by one parameter (θ).

denotes the annihilation operator of the j^{th} output mode. Then, in the Heisenberg picture, the transformation provided by the beam splitter reads

$$\begin{pmatrix} \hat{a}_{1,\text{OUT}} \\ \hat{a}_{2,\text{OUT}} \end{pmatrix} = \begin{pmatrix} \cos \theta & \sin \theta \\ -\sin \theta & \cos \theta \end{pmatrix} \begin{pmatrix} \hat{a}_{1,\text{IN}} \\ \hat{a}_{2,\text{IN}} \end{pmatrix}. \quad (2.13)$$

It is evident from (2.13) that both output modes are coherent superpositions of input modes. Because of the coherent nature of this coupling on the beam splitter, output modes can manifest interference that is often exploited in quantum state engineering.

It is also possible to describe the action of a beam splitter in the Schrödinger picture. Using this picture, we represent the beam splitter by the Hamiltonian

$$\hat{H}_{\text{BS}} = i\theta(a_1 a_2^\dagger - a_1^\dagger a_2). \quad (2.14)$$

The transformation performed by the beam splitter on incident state of light is then described by evolution operator generated by the Hamiltonian (2.14).

The phenomenon of photon bunching can be observed using balanced beam splitter ($\theta = \pi/4$). If a pair of photons arrives at the balanced beam splitter and each photon arrives by different input mode, we observe interference between these two photons. This phenomenon is called Hong-Ou-Mandel interference and it leads to coherent superposition of two photons in the first output mode and two photons in the second output mode. This process can be schematically written in the form of

$$|1_1, 1_2\rangle \longrightarrow \frac{1}{\sqrt{2}} (|2_1, 0_2\rangle + |0_1, 2_2\rangle), \quad (2.15)$$

where numbers in brackets denote the number of photons and subscripts label the mode. First experimental demonstration of this effect has been performed by C. K. Hong, Z. Y. Ou and L. Mandel in 1987 [82].

2.2.2 Phase shifter

The phase shifter is a one-mode optical component characterized by one real parameter φ that provides capability to adjust phase of light. There are several ways to control the phase shift. One may use movable mirrors and vary the phase shift by changing the trajectory length of light. Another possibility is to control optical thickness by using a suitably thin transparent glass plate. The phase shifter is often used to manipulate phase difference between two modes by shifting one of them (see fig. 2.2). As in the case of the beam splitter, modes are described

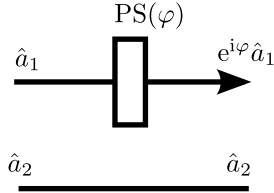


Figure 2.2: Phase shifter characterized by one parameter (φ) is acting on one mode.

by annihilation operators. The phase shifter causes the annihilation operator of the first mode to transform

$$\hat{a}_1 \longrightarrow e^{i\varphi} \hat{a}_1. \quad (2.16)$$

If there is one photon in the phase shifted mode, it gets shifted by the amount of $e^{i\varphi}$. If there are two photons, then the phase shift is twice as large ($e^{2i\varphi}$) and so on. Mode in vacuum state is not affected by the phase shifter operation.

As in the case of the beam splitter, one may describe the action of the phase shifter using the effective Hamiltonian

$$\hat{H}_{\text{PS}} = \varphi \hat{a}^\dagger \hat{a}. \quad (2.17)$$

2.2.3 Polarizing beam splitter

This device is very similar to the normal beam splitter. It transmits a specified portion of light and reflects the rest. It differs from the ordinary beam splitter by its sensitiveness to polarization. An ideal polarising beam splitter entirely reflects horizontally polarized light and entirely transmits the vertically polarized one. A general polarizing beam splitter has independent transmitivities for horizontal and for vertical polarization. Polarising beam splitter can be even imagined as two ordinary beam splitters in one, one for horizontal and one for vertical polarization. It mixes two input beams into two output beams for horizontal and for vertical polarization independently (see fig. 2.3), because these two polarizations do not interact one with the other. Effectively it is a four-mode transformation device. The po-

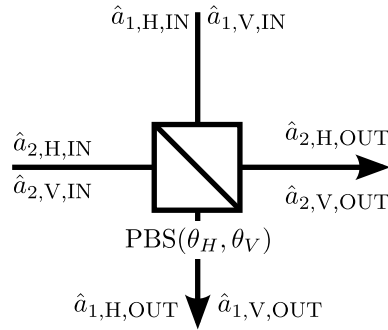


Figure 2.3: Polarizing beam splitter can be understood as two ordinary beam splitters in one acting on horizontal and vertical polarization separately. The number of characterizing parameters is two - each for one polarization.

larizing beam splitter can therefore be described using two parameters (θ_H, θ_V) with similar meaning as in the case of an ordinary beam splitter. First parameter corresponds to horizontal polarization and the second to the vertical one. Corresponding transformation matrix for annihilation operators reads

$$\begin{pmatrix} \hat{a}_{1H,OUT} \\ \hat{a}_{1V,OUT} \\ \hat{a}_{2H,OUT} \\ \hat{a}_{2V,OUT} \end{pmatrix} = \begin{pmatrix} \cos \theta_H & 0 & \sin \theta_H & 0 \\ 0 & \cos \theta_V & 0 & \sin \theta_V \\ -\sin \theta_H & 0 & \cos \theta_H & 0 \\ 0 & -\sin \theta_V & 0 & \cos \theta_V \end{pmatrix} \begin{pmatrix} \hat{a}_{1H,IN} \\ \hat{a}_{1V,IN} \\ \hat{a}_{2H,IN} \\ \hat{a}_{2V,IN} \end{pmatrix}, \quad (2.18)$$

where subscript H denotes horizontal polarization and V vertical polarization.

2.2.4 Half-wave plate

Half-wave plate is an optical component serving to alter polarization state of the light beam. It is made of an uniaxial anisotropic crystal with optical axis oriented perpendicularly to propagation direction of the light beam. If linearly polarized light passes through the half-wave plate, its polarization remains linear, but rotates by the angle

$$\varphi = 2\alpha, \tag{2.19}$$

where α is the angle between initial polarization direction and the direction of optical axis of the plate. In this work, half-wave plates are used to switch horizontal and vertical linear

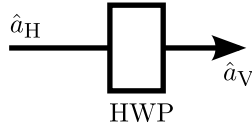


Figure 2.4: Half-wave plate with its optical axes oriented diagonally. Its effect on horizontal polarization is to switch it to vertical polarization.

polarizations (see fig. 2.4). For this purpose, the half-wave plate is rotated diagonally, so that the angle α is $\pi/4$. Transformation performed by this particular configuration of half-wave plate can be written as

$$\hat{a}_H \longrightarrow \hat{a}_V \quad \text{and} \quad \hat{a}_V \longrightarrow \hat{a}_H. \tag{2.20}$$

Circular polarization is switched from right-handed to left-handed and vice-versa every time it passes through the half-wave plate. In this case, there is not any specific angle to set for this transformation to be done.

2.2.5 Light squeezing

It has been demonstrated that even the ground (or vacuum) state of light contains some energy, $\frac{1}{2}\hbar\omega$ to be precise. This energy causes fluctuations if we measure quadratures of light (see fig. 2.5). These fluctuations are centered at origin $x, p = 0$ and in the pure vacuum state $|0\rangle$ they are circularly symmetrical. Due to commutation relations between quadrature operators and Heisenberg uncertainty principle, these fluctuations are irreducible. We can however reduce fluctuations in one quadrature at the expense of amplifying fluctuations in

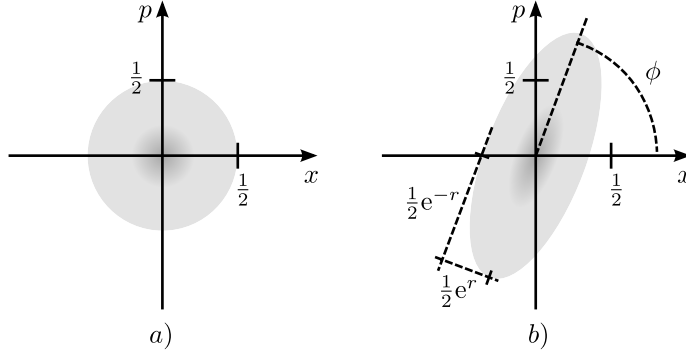


Figure 2.5: Vacuum fluctuation of the pure vacuum state (a) and of the squeezed vacuum state (b). The squeezing is performed by the squeezing operator as defined by (2.21).

orthogonal quadrature. Such quantum state is then called squeezed state. If the squeezing operation is performed on vacuum state, one obtains the so-called squeezed vacuum.

Squeezing operation can be described by the so-called squeezing operator

$$\hat{S}(\xi) = \exp\left(\frac{\xi^*}{2}\hat{a}^2 - \frac{\xi}{2}\hat{a}^{\dagger 2}\right), \quad (2.21)$$

where

$$\xi = -re^{i\phi} \quad (2.22)$$

is a complex parameter. Amplitude r of ξ determines how big the squeezing is and the phase ϕ defines in which direction (or angle) the squeezing is performed. In Heisenberg picture, one can write transformation of quadrature operators due to the squeezing (in this case with $\phi = 0$ and vacuum as initial state)

$$\hat{x} \longrightarrow e^r \hat{x} \quad \text{and} \quad \hat{p} \longrightarrow e^{-r} \hat{p}. \quad (2.23)$$

We see, that one quadrature is squeezed and the orthogonal quadrature is anti-squeezed. In the Schrödinger picture, similar transformation can be written for the wave function in \hat{x} or \hat{p} representation.

The minimum value of product of two conjugated quadrature variances is determined by the Heisenberg uncertainty principle. The overall variance can not be suppressed, however one can lower the variance of one quadrature at the expense of getting the variance of the conjugated quadrature higher.

To perform the squeezing, one needs to find a device whose Hamiltonian is in the form of (2.21). Optical parametric amplifier (OPA) is one example of such device and the process provided by it is called the parametric down-conversion. The OPA consists of a non-linear optical crystal placed inside an optical resonator. Strong coherent beam is used to pump optical energy into the device. Correct phase matching and resonator setting assures that the action of the optical parametric amplifier is described by the Hamiltonian in the form of (2.21). During the process of parametric down-conversion, one photon of the pumping beam decays into two photons with lower frequencies called the signal photon and the idler photon. The sum of their frequencies is constant and it is equal to the frequency of the pump beam. Signal and idler photons therefore manifest anticorrelations in their frequencies. It is possible to stimulate the process of parametric down-conversion by injecting some initial signal to the signal mode. Another possibility is to proceed with vacuum initial state in the signal and idler mode and let the pumping beam pass only once through the non-linear medium. Such process is called spontaneous parametric down-conversion and it is considered in this thesis as a source of pairs of photons in polarization entangled state.

2.3 Quantum non-demolition interaction

It is a well known fact that quantum measurement disturbs the state of the measured system. As an example we may consider detection of a photon by APD. Such measurement allows us to detect presence of a photon, but in the process of detection this photon is destroyed. It is therefore impossible to use such technique to simply detect a photon and use it later in some experiment. Usually we need to resort to post-selection, so that the measurement is effected at the output of an experiment and we just post-select favorable cases.

A very important procedure is the so-called quantum non-demolition (QND) interaction. The general idea is to exploit an interaction between two systems during which some property of one system (called the signal) is “written” into the second system (called the meter).

The QND interaction is employed in the present thesis to prepare the Dicke states of atoms. For this reason, we will discuss the QND interaction between light and atoms as it is used later on. Quantum state of an atomic ensemble can be described using collective atomic

spin operators \hat{S}_x , \hat{S}_y and \hat{S}_z that satisfy commutation relation

$$[\hat{S}_y, \hat{S}_z] = i\hat{S}_x. \quad (2.24)$$

By making the expectation value of \hat{S}_x sufficiently large, e.g. by optical pumping, the other two collective spin operators manifest similar algebraic properties as quadrature operators of light

$$[\hat{S}_y, \hat{S}_z] \propto i\langle \hat{S}_x \rangle. \quad (2.25)$$

This similarity can be exploited to define the quadrature operators \hat{x}_A and \hat{p}_A for atoms as well

$$\hat{x}_A = \frac{\hat{S}_y}{\sqrt{2\langle \hat{S}_x \rangle}} \quad \text{and} \quad \hat{p}_A = \frac{\hat{S}_z}{\sqrt{2\langle \hat{S}_x \rangle}}. \quad (2.26)$$

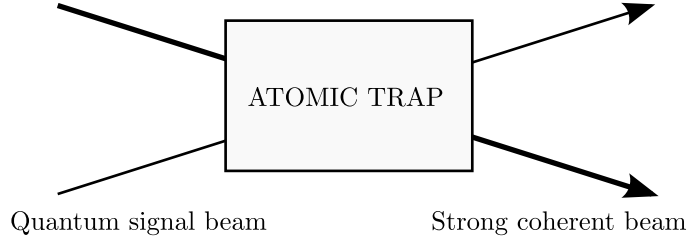


Figure 2.6: Quantum non-demolition interaction between light and atoms.

To perform the QND interaction, we hold the atoms in a trap or in a glass cell as shown in figure 2.6. To assure the interaction of atomic spin with light, we fire a laser beam through the trap. The laser beam consists of a strong linearly polarized coherent part and a quantum signal, that is orthogonally polarized. Using quadrature operators as the description for both light and atoms, we can write the effective interaction Hamiltonian in the form of

$$\hat{H}_{\text{QND}} = \bar{\kappa} \hat{x}_L \hat{x}_A, \quad (2.27)$$

where $\bar{\kappa}$ denotes the interaction constant and subscripts A and L are used for atomic and light quadrature operators respectively.

In Heisenberg picture, this interaction leads to evolution of quadrature operators of atoms

and light

$$\begin{aligned}
\hat{x}_A &\longrightarrow \hat{x}_A \\
\hat{x}_L &\longrightarrow \hat{x}_L \\
\hat{p}_A &\longrightarrow \hat{p}_A + \kappa\hat{x}_L \\
\hat{p}_L &\longrightarrow \hat{p}_L + \kappa\hat{x}_A,
\end{aligned}
\tag{2.28}$$

where $\kappa = \frac{\bar{\kappa}t}{2\hbar}$, t being the effective interaction time. We notice that both \hat{x} quadratures of atoms and light remain unchanged and are therefore not destroyed. As for the \hat{p} quadratures, we notice, that they are “recording” information on the \hat{x} quadratures of their counterparts. This is the writing process mentioned above. Measurement of \hat{p}_L allows to measure \hat{x}_A in a non-demolition way.

2.4 Detection of light

For the schemes in the present work to be successful and to be verified, one needs to be able to detect and recognize various states of light. It is therefore useful to discuss some light detection techniques used in later proposed schemes.

2.4.1 Single photon detection

It is possible to detect one photon using the so-called avalanche photodiodes (APD). These devices are similar to ordinary photodiodes, but high reverse bias voltage is applied on them. Energy of one photon is then sufficient to cause a breakdown followed by the so-called avalanche of electrical current which can be detected. The efficiency of APD is not nearly 100% and this the reason why non-detection, or detection of vacuum is not possible with high fidelity in the experimental reality. Even when the detector detects a photon (we call this event the click of a detector), we are not sure that only one photon has been present in the detected mode or whether two or more photons impinged on the detector. APD distinguishes only between presence and absence of photons in the field and can be therefore described by a two-component POVM consisting of projectors onto vacuum and on the rest of the Hilbert space

$$\hat{\Pi}_{\text{CLICK}} = \hat{\mathbb{1}} - |0\rangle\langle 0|, \quad \hat{\Pi}_{\text{NO CLICK}} = |0\rangle\langle 0|.
\tag{2.29}$$

There are some techniques to obtain a photon number resolving detector whose operation can be described by

$$\hat{\Pi}_n = |n\rangle\langle n| \quad (2.30)$$

and which is capable of measuring the actual number of photons in the mode. The performance of these detectors is however significantly limited by the relatively low detection efficiency.

2.4.2 Homodyne detection

In the beginning of this chapter, we have defined the quadrature operators of light \hat{x} and \hat{p} . One may be curious, if there is a possibility to measure these operators. The answer is yes and it may be achieved using the homodyne detection (see fig. 2.7).

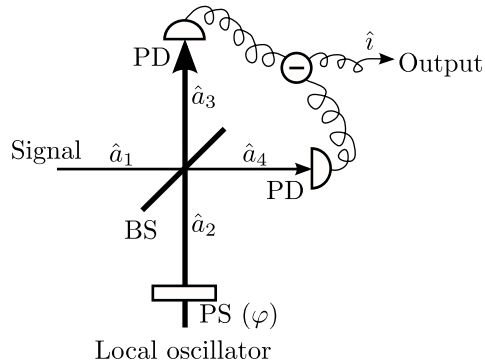


Figure 2.7: Homodyne detection. Signal and local oscillator are mixed on the balanced beam splitter BS, both output ports are then measured by photodiodes PD. Resulting photocurrents are subtracted and the outcome corresponds to the measured value of signal quadrature depending on the phase shift φ imposed by the phase shifter PS.

This technique consists of a signal beam, a strong coherent beam called the local oscillator at the same frequency as the signal beam, a balanced beam splitter and two photodiodes. Phase difference φ between local oscillator and signal can be set using a phase shifter. Local oscillator and the signal interfere on the balanced beam splitter BS. The outgoing modes can be expressed in the form of

$$\hat{a}_3 = \frac{1}{\sqrt{2}} (\hat{a}_1 + e^{i\varphi} \hat{a}_2) \quad \text{and} \quad \hat{a}_4 = \frac{1}{\sqrt{2}} (\hat{a}_1 - e^{i\varphi} \hat{a}_2). \quad (2.31)$$

Photodiodes detect signal corresponding to $\hat{a}_3^\dagger \hat{a}_3$ and $\hat{a}_4^\dagger \hat{a}_4$ and convert it to photocurrents. Electronic device can perform subtraction of these photocurrents

$$\hat{i} = \hat{a}_3^\dagger \hat{a}_3 - \hat{a}_4^\dagger \hat{a}_4 \quad (2.32)$$

and the outcome is the value of a certain quadrature operator depending on the phase shift imposed by the phase shifter

$$\hat{i} \approx \hat{a}_1 e^{-i\varphi} + \hat{a}_1^\dagger e^{i\varphi}, \quad (2.33)$$

where the approximation of strong coherent beam has been employed ($\hat{a}_2 \rightarrow \alpha_2$).

2.5 Numerical simulations

To verify the functionality of the schemes proposed in this thesis, I have carried out several numerical simulations. These simulations are programmed in a high-level mathematical language and run by Matlab or GNU Octave. Source codes of these simulations are available on the CD attached to the printed version of this theses. The source codes may be freely used under the terms of the GPL.

Chapter 3

Preparation of two-photon entangled states in several spatial modes

3.1 Introduction

In this chapter, we show that we can exploit experimentally accessible two-photon entangled states generated in the process of spontaneous parametric down-conversion to extend the group of states that can be prepared using only passive linear optics and single-photon detectors. We propose a feasible protocol for generation of an arbitrary quantum state of two photons in three optical spatial modes

$$|\psi_{\text{target}}\rangle = \alpha|200\rangle + \beta|020\rangle + \gamma|002\rangle + \delta|110\rangle + \epsilon|101\rangle + \eta|011\rangle, \quad (3.1)$$

where the numbers in each bracket denote the number of photons in the first, second and third mode, respectively. The text of this chapter is based on our published article [83]. To prepare an arbitrary state (3.1) we use a multiphoton interferometer, which is schematically shown in Fig. 3.1. A two-mode two-photon state can be prepared in this way from a separable state $|110\rangle$ as the input. This approach however fails if the number of modes becomes higher. We will show that using an entangled input state permits us to create arbitrary states of the form (3.1). We will then generalize our procedure to conditional generation of arbitrary multi-mode

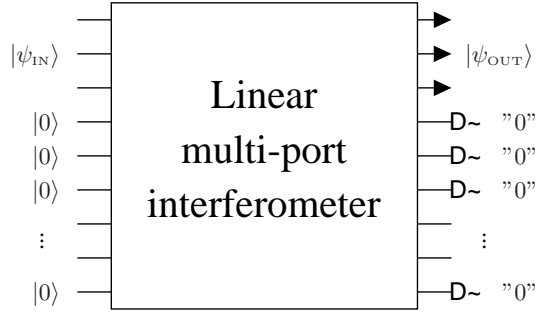


Figure 3.1: General multiphoton interferometer transforming a three-mode input state $|\psi_{\text{in}}\rangle$ into $|\psi_{\text{out}}\rangle$ using only vacuum ancillae. We post-select cases when both photons are present in the first three output modes.

entangled two-photon state. The scheme is cheap in terms of required resources because it involves only two photons and vacuum ancillae which is a great practical advantage.

The rest of this chapter is organized as follows. In Sec. 3.2 we prove that separable input two-photon state is insufficient for generation of arbitrary multimode two-photon state via interference and post-selection. In Sec. 3.3 we describe the scheme for generation of arbitrary three-mode states (3.1). Results of numerical simulations of generation of various states are presented in Sec. 3.4. In Sec. 3.5 we generalize the state preparation procedure to arbitrary number of modes. A simple experimentally feasible scheme tailored for generation of a specific class of four-mode two-photon states, the so-called KLM states, is discussed in Sec. 3.6. Finally, Sec. 3.7 contains a brief summary of the main results and conclusions.

3.2 Motivation

First of all we prove that a separable input state is not sufficient for preparation of an arbitrary state of the form (3.1) by the interferometric method sketched in Fig. 3.1. We express the input state $|110\rangle$ as $\hat{a}_1^\dagger \hat{a}_2^\dagger |\text{vac}\rangle$, where \hat{a}_i^\dagger denotes creation operator for the i^{th} mode and $|\text{vac}\rangle$ stands for the vacuum state. General interferometer performs linear transformation that can be written as

$$\hat{a}_{i,\text{in}}^\dagger = \sum_j u_{ij} \hat{a}_{j,\text{out}}^\dagger, \quad (3.2)$$

where $u_{ij} \in \mathbb{C}$ are elements of a unitary matrix U . For future reference, we note that the interference of modes a and b on a beam splitter BS with amplitude transmittance t and reflectance $r = \sqrt{1 - t^2}$ is governed by

$$a_{\text{out}}^\dagger = ta_{\text{in}}^\dagger + rb_{\text{in}}^\dagger, \quad b_{\text{out}}^\dagger = tb_{\text{in}}^\dagger - ra_{\text{in}}^\dagger, \quad (3.3)$$

and a phase shifter PS shifts the phase of a single mode according to $a_{\text{out}}^\dagger = e^{i\phi}a_{\text{in}}^\dagger$. The separable state $|110\rangle$ will be transformed as follows,

$$|110\rangle \rightarrow \left(\sum_j u_{1j} a_{j,\text{out}}^\dagger \right) \left(\sum_k u_{2k} a_{k,\text{out}}^\dagger \right) |\text{vac}\rangle. \quad (3.4)$$

Conditional projection of all output ancillae onto vacuum then gives

$$|110\rangle \rightarrow \left(\sum_{j=1}^3 u_{1j} a_{j,\text{out}}^\dagger \right) \left(\sum_{k=1}^3 u_{2k} a_{k,\text{out}}^\dagger \right) |\text{vac}\rangle. \quad (3.5)$$

It is easy to verify that the class of achievable target states (3.5) is limited. For example it can be shown that the state

$$|110\rangle + |101\rangle + |011\rangle = (a^\dagger b^\dagger + a^\dagger c^\dagger + b^\dagger c^\dagger) |\text{vac}\rangle \quad (3.6)$$

cannot be expressed in the factorized form (3.5) and is therefore not obtainable from separable state like $|110\rangle$ by multiphoton interference using only vacuum ancillae. Addition of single photon ancillae would make the preparation possible, but also experimentally more difficult [84].

Even with one fixed entangled state as the input, one can not prepare arbitrary state (3.1) using only deterministic unitary transformations. To prove this, let us consider two photons in n optical modes. Such quantum state is then determined by

$$2R_2^n - 2 = n^2 + n - 2 \quad (3.7)$$

real parameters where $R_k^n = \binom{n+k-1}{k}$ denotes the number of combinations with repetitions of n elements in k classes. The term -2 corrects the number of parameters due to normalization and irrelevant overall phase of the state. On the other hand, n -dimensional special unitary transformation represented by $n \times n$ complex matrix contains

$$2n^2 - n - 2C_2^n - 1 = n^2 - 1 \quad (3.8)$$

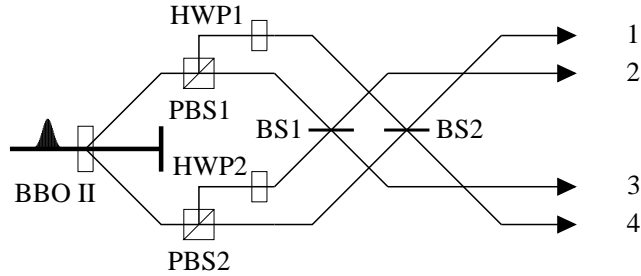


Figure 3.2: Initialization phase of the protocol. Pair of photons obtained by spontaneous parametric down-conversion in a nonlinear crystal BBO is sent to polarizing beam splitters PBS1 and PBS2 which transmit horizontally polarized photons and reflect vertically polarized photons. Half wave plates HWP1 and HWP2 are inserted to modes 2 and 3 to align the polarization of all beams to vertical. The photons then interfere on two ordinary balanced beam splitters BS1 and BS2.

real parameters, where $C_k^n = \binom{n}{k}$ denotes the number of combinations without repetitions of n elements in k classes. The factor $-n$ in Eq. (3.8) accounts for the reduction of the number of free parameters due to normalization condition of each row of the matrix. The term $-2C_2^n$ represents correction due to condition of orthogonality of rows and the factor -1 occurs since the determinant of a matrix belonging to the $SU(n)$ group is fixed and equal to 1. It is evident that for any $n > 1$ the number of parameters specifying the quantum state is larger than the number of degrees of freedom allowed by unitary transformation. This results in the need of probabilistic non-unitary filtering operations in a fully general preparation scheme.

3.3 Preparation scheme

Here we show that by exploiting the two-photon entangled states generated by spontaneous parametric down-conversion as a resource, we can conditionally generate arbitrary state of the form (3.1) with only linear optics. The protocol can be divided in two phases: initialization phase and preparation phase. We begin by describing the first one.

3.3.1 Initialization phase

We use spontaneous parametric down-conversion to prepare an entangled pair of photons (see Fig. 3.2). The initial state of these photons can be written as

$$|\psi\rangle = \frac{1}{\sqrt{2}} (|HV\rangle + |VH\rangle), \quad (3.9)$$

where H and V denote state of single photon polarized horizontally or vertically, respectively. Using two polarizing beam splitters that reflect vertical and transmit horizontal polarization we are able to obtain the four-mode state

$$|\psi\rangle = \frac{1}{\sqrt{2}} (|1001\rangle + |0110\rangle), \quad (3.10)$$

where the Fock state basis is used. Four numbers in each bracket denote the number of photons found in spatial modes 1 through 4, respectively. Half-wave plates HWP1 and HWP2 unify polarization states in all four modes. Then the Hong-Ou-Mandel interference [82] takes place on balanced beam splitters BS1 and BS2 and the state of the photons changes to

$$|\psi\rangle = \frac{1}{2} (|2000\rangle + |0200\rangle + |0020\rangle + |0002\rangle). \quad (3.11)$$

If we want to generate a three-mode state, then we simply omit the last mode. Since in our protocol we post-select cases when two photons are present at the output of the preparation device, we can assume the effective initial two-photon state in the form

$$|\psi\rangle = \frac{1}{\sqrt{3}} (|200\rangle + |020\rangle + |002\rangle), \quad (3.12)$$

which will be used in the second phase of the protocol.

3.3.2 Preparation phase

In order to prepare an arbitrary state (3.1) the state (3.12) is fed into a multiport linear interferometer schematically illustrated in Fig. 3.3. The device is composed of passive linear optical elements such as beam splitters and phase shifters and involves filters F1 and F2 where the signal beams are attenuated by mixing them with auxiliary vacuum beams on beam splitters. The filtering operation is successful if the photons do not leak into the output auxiliary ports. This can be, in principle, verified by means of single-photon detectors placed

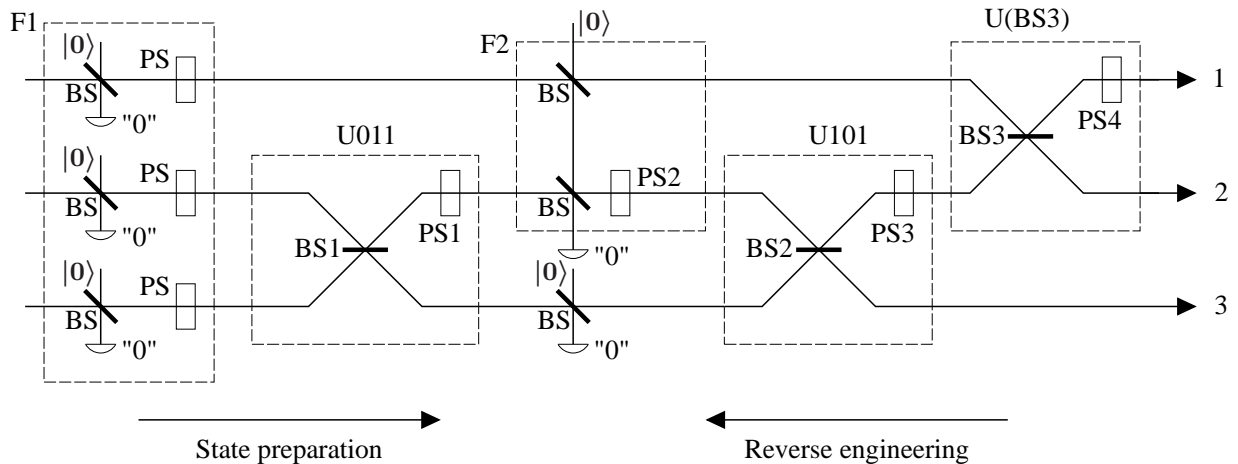


Figure 3.3: Preparation phase. The linear interferometer involves three unitary operations U_{011} , U_{101} and $U(\text{BS3})$ composed of beam splitters BS_j and phase shifters PS_k . The preparation also requires two attenuation filters F_1 and F_2 which are implemented using unbalanced beam splitters and vacuum ancillae. Successful filtration can be verified by monitoring the output ancilla modes with single-photon detectors. In the design of the scheme we imagine reverse propagation of the state backwards from the output to the input.

on the auxiliary outputs, as shown in Fig. 3.3. However, such verification would require perfect detectors with unit efficiency. Instead, we can utilize a simpler verification strategy relying on postselection. To prove that the scheme is working, one can set detectors on every output mode and look for double coincidences which herald successful preparation of the state. Quantum state tomography [85] could be used to completely characterize the generated state. In this case the target state is destroyed by the measurement. If the prepared state serves as an input for another scheme, one can post-select successful preparations at the output of such scheme.

The parameters of the interferometer elements can be determined by “reverse engineering” of the target state. We let the target state propagate through the scheme in reverse and we successively get rid of all terms but the terms that are present in the state (3.12). The reversal is easily done for beam splitters (BS_1 , BS_2 and BS_3) and phase shifters (PS_1 , PS_2 and PS_3) because they are represented by unitary transformations. Filters F_1 and F_2 are also (probabilistically) reversible. Once the reverse procedure finds correct parameters for all elements, the scheme is designed to generate the target state (3.1) from the state (3.12).

In the Heisenberg picture, passive linear transformations can be described as linear unitary

transformations of the creation operators, c.f. Eq. (3.2). Every three-mode transformation can be decomposed into a sequence of two-mode and single-mode transformations corresponding to beam splitters and phase shifters [86]. A fully general interferometric scheme can thus be constructed from these basic building blocks. Such a device would provide a large number of degrees of freedom that can be exploited to optimize the success probability of the state preparation but at the same time its experimental realization would be quite difficult. We have therefore chosen some sort of compromise. Our scheme includes all necessary elements needed for the preparation of arbitrary state (3.1) and one additional beam splitter BS3 and phase shifter PS4 as optional optimization elements. These components can be removed and our scheme thus simplified at the expense of a reduced probability of successful state preparation.

In what follows we imagine that the state propagates backwards through the scheme from the right to the left. We successively eliminate all terms where two photons are present in two different spatial modes and end up with the state (3.12) as a result. First of all we get rid of the cross term $|101\rangle$ with complex amplitude ϵ by destructive interference. To this end, we employ a unitary transformation U101 represented by a beam splitter BS2 with amplitude transmittance τ_2 accompanied by phase shifter PS3 imposing phase shift ϕ_3 . By a simple calculation, one finds that setting $\phi_3 = -\arg \delta + \arg \epsilon$ and $\tau_2 = \frac{u}{\sqrt{1+u^2}}$, where $u = \left|\frac{\epsilon}{\delta}\right|$, the state $|101\rangle$ is completely eliminated by destructive interference.

The success rate of the protocol can be increased by the optimization beam splitter BS3 mixing modes 1 and 2. Amplitude transmissivity τ_3 of BS3 should be chosen such that in the reverse propagation after transformation U101 the amplitude of the state $|110\rangle$ is minimized. The optimal value of τ_3 can be found numerically by a simple computer algorithm that maximizes the overall probability of success of the protocol. The reverse propagated state impinging on the filter F2 from the right can be written as

$$|\psi'\rangle = \alpha'|200\rangle + \beta'|020\rangle + \gamma'|002\rangle + \delta'|110\rangle + \eta'|011\rangle. \quad (3.13)$$

If the term $|110\rangle$ is not completely eliminated and $\delta' \neq 0$ we are forced to employ a filter F2 in modes 1 and 2. Let \hat{a}^\dagger and \hat{b}^\dagger denote the creation operators for modes 1 and 2, respectively.

The filtration by F2 can be expressed as

$$\begin{pmatrix} \hat{a}_{\text{out}}^\dagger \\ \hat{b}_{\text{out}}^\dagger \end{pmatrix} = \begin{pmatrix} q_2 & -\frac{\delta' q_2}{\alpha' \sqrt{2}} \\ 0 & q_2 \end{pmatrix} \begin{pmatrix} \hat{a}_{\text{in}}^\dagger \\ \hat{b}_{\text{in}}^\dagger \end{pmatrix}, \quad (3.14)$$

where q_2 is set so that the matrix can make part of a bigger unitary transformation on three modes. Without loss of any generality we can assume that δ'/α' is real and positive because the phase shift between the two amplitudes is compensated by the phase shifter PS2 if we set $\phi_2 = \arg \alpha' - \arg \delta'$. The amplitude transmittance of the beam splitters forming the filter F2 is equal to q_2 . The correct mixing of modes is achieved if the product of the amplitude reflectances $1 - q_2^2$ of the two beam splitters is equal to $-\delta' q_2 / \sqrt{2} \alpha'$. This yields a quadratic equation for q_2 whose solution reads

$$q_2 = \frac{1}{2} \left[\frac{\delta'}{\sqrt{2} \alpha'} - \sqrt{\left(\frac{\delta'}{\sqrt{2} \alpha'} \right)^2 + 4} \right]. \quad (3.15)$$

The filtering requires an ancilla vacuum mode and the transformation (3.14) is effectively implemented if no photon leaks into the output ancilla. Note that Eq. (3.14) does not preserve canonical commutation relations because the operator of ancilla mode is omitted. This simplified mathematical description of the filter is nevertheless correct for our purposes.

After filter F2 the state simplifies to

$$|\psi''\rangle = \alpha''|200\rangle + \beta''|020\rangle + \gamma''|002\rangle + \eta''|011\rangle. \quad (3.16)$$

To ensure correct state preparation, one has to compensate filtering of modes 1 and 2 by additional attenuation of the third mode by a beam splitter with amplitude transmissivity q_2 . The probability of success P_{F2} of the filter F2 can be lower bounded as follows. The successful filtration during the state preparation procedure can be described by the transformation $|\psi'\rangle = M|\psi''\rangle$, where the non-unitary operator M depends on q_2 . We have $P_{F2} = \langle \psi'' | M^\dagger M | \psi'' \rangle / \langle \psi'' | \psi'' \rangle$ from which we obtain the inequality $P_{F2} \geq m_{\min}$ where m_{\min} is the lowest eigenvalue of the matrix $M^\dagger M$. A straightforward calculation yields

$$m_{\min} = \frac{1}{2} [q_2^4 + (1 - q_2^2 + q_2^4)^2] - \frac{1}{2} (1 - q_2^2)^2 \sqrt{1 + 6q_2^4 + q_2^8}. \quad (3.17)$$

It can be shown that m_{\min} is a monotonically increasing function of q_2 which suggests that in order to maximize the success rate of the protocol we should maximize q_2 . It follows from Eq.

(3.15) that q_2^2 monotonically decreases as the ratio δ'/α' increases. It is therefore desirable to minimize δ' and maximize α' which is precisely the purpose of the beam splitter BS3. Let us now derive a lower bound on q_2^2 . The maximum of absolute values of the amplitudes specifying the state (3.1) is greater or equal to $1/\sqrt{6}$. If the maximum amplitude corresponds to one of the states with two photons in a single mode then by simple relabeling of the modes we get $\alpha' \geq 1/\sqrt{6}$. If this amplitude corresponds to mode with two photons in two different modes, say $|110\rangle$ after possible re-labeling, then we may use balanced beam splitter BS3 together with proper phase shifts to reach amplitude $\alpha' \geq 1/\sqrt{12}$. Since the unitary operations U(BS3) and U101 are deterministic, the state (3.13) is normalized and $|\alpha'|^2 + |\delta'|^2 \leq 1$ which implies $|\delta'| \leq \sqrt{\frac{11}{12}}$. Taking everything together, we find that $|\delta'/\alpha'| \leq \sqrt{11}$ can always be satisfied so that $q_2^2 \geq (15 - \sqrt{209})/4 \approx 0.136$ holds. If we plug in this lower bound into Eq. (3.17) we finally get $P_{F2} \geq 0.52\%$.

In the next step of the protocol, the term $\eta''|011\rangle$ in the state (3.16) is removed by a destructive interference between second and third modes. This is accomplished by a unitary transformation U011 which consists of a phase shifter PS1 imposing phase shift ϕ_1 on the second mode and a beam splitter BS1 with transmittance $\tau_1 = \cos \vartheta$ mixing the second and third mode. The term $\eta''|011\rangle$ is eliminated provided that

$$\begin{aligned} \tan \phi_1 &= \frac{\text{Im}[(\gamma'' - \beta'')/\eta'']}{\text{Re}[(\gamma'' + \beta'')/\eta'']}, \\ \tan(2\vartheta) &= \frac{\sqrt{2}\eta''}{e^{-i\phi_1}\gamma'' - e^{i\phi_1}\beta''}, \end{aligned} \tag{3.18}$$

After the whole procedure we obtain the state

$$|\psi'''\rangle = \alpha'''|200\rangle + \beta'''|020\rangle + \gamma'''|002\rangle, \tag{3.19}$$

which can be transformed by filters F1 into the state (3.12). We denote by P_{F1} the overall success probability of filters F1. In order to obtain the state (3.19) from the initial state (3.12) we in fact need to apply attenuation filters to only two modes. With probability $\frac{1}{3}$ the two photons are present in a mode which is not attenuated by F1 and, consequently, it holds that $P_{F1} \geq \frac{1}{3}$.

Parameters of all components are now determined. By proper inversion of the filters we obtain configuration which prepares the target state (3.1) from the state (3.12). The total

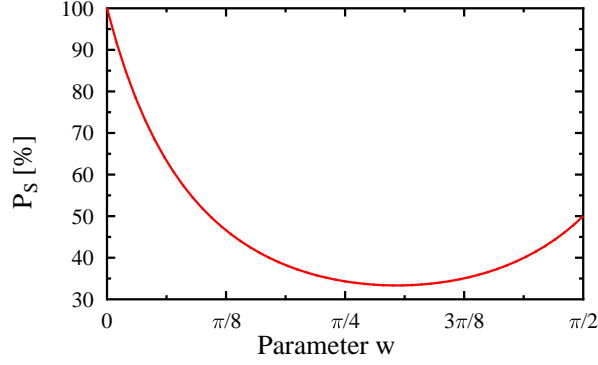


Figure 3.4: Success probability P_S of the protocol for states (3.21) is plotted as a function of the parameter $w \in [0; \frac{\pi}{2}]$.

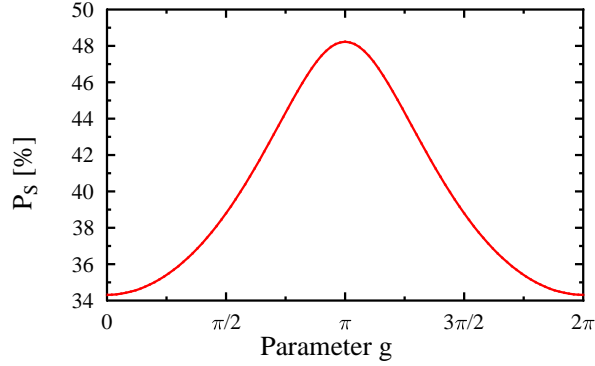


Figure 3.5: Success probability P_S of the protocol for states (3.22) is plotted as a function of the phase shift $g \in [0, 2\pi]$.

success probability for the whole protocol is defined as

$$P_S = \langle \psi_{\text{OUT}} | \psi_{\text{OUT}} \rangle, \quad (3.20)$$

where $|\psi_{\text{OUT}}\rangle$ is un-normalized output state obtained from the normalized input state (3.12).

It holds that $P_S = P_{F1}P_{F2} \geq 0.17\%$.

3.4 Numerical simulations

To verify the functionality of our protocol, we have performed extensive numerical simulations of preparation of various states. An example of the results is given in Fig. 3.4 which displays

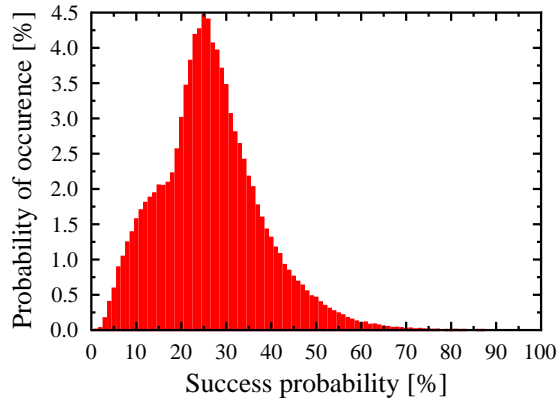


Figure 3.6: Success probability histogram. For a given randomly generated set of 10^5 states, the minimum success probability of the scheme reads 0.69%. The average success probability is around 26.0%.

the probability of successful preparation for target states

$$|\psi_1\rangle \propto \cos w (|200\rangle + |020\rangle + |002\rangle) + \sin w (|110\rangle + |101\rangle + |011\rangle), \quad (3.21)$$

where $w \in [0, \frac{\pi}{2}]$. We can see that as w increases the target state is “shifting off” the state (3.12) which is the product of the initialization phase. Even though the probability decreases, it is still well above 30%. It can be shown that for this particular class of states the best performance of the protocol is obtained by using a balanced optimizing beam splitter BS3. This probability P_S is however very sensitive to exact splitting ratio of the beam splitter when $w \approx 0.3\pi$. In this case it is therefore more convenient for the experimental realization to use an unbalanced beam splitter with splitting ratio that corresponds to another local maximum of the success probability. Even though this choice gives a slightly lower success probability, it makes the scheme more robust and tolerant to imprecisions in the splitting ratio.

In another numerical simulation we have studied preparation probability P_S for a more asymmetric single-parametric class of states

$$|\psi_2\rangle \propto |200\rangle + |101\rangle + |002\rangle + e^{gi}(|110\rangle + |020\rangle + |011\rangle), \quad (3.22)$$

where $g \in [0, 2\pi]$. The result (see Fig. 3.5) shows a symmetric Gauss-like function achieving maximum of 48% at $g = \pi$ and asymptotically approaching minimum of 34% for $g = 0, 2\pi$.

Finally, we present in Fig. 3.6 a histogram of the success probability P_S of the preparation protocol. This histogram was obtained by evaluating P_S for 10^5 randomly generated states. We can see that most of the states can be prepared with probability larger than 15%. However, there is a small class of states that are hard to generate. The lowest success probability obtained by the numerical calculations reads 0.69% which qualitatively agrees with the lower bound 0.17% derived in the preceding section.

3.5 Generalization to an arbitrary number of modes

So far we have explained how linear optics can be used to prepare an arbitrary state of two photons in three spatial modes. We now generalize our procedure to an arbitrary number of modes. Figure 3.7 schematically depicts the scheme for preparation of an arbitrary two-photon state of the form

$$|\psi_{\text{target}}\rangle = \sum_{j=1}^N \alpha_j |2_j\rangle + \sum_{j,k=1, j \neq k}^N \beta_{jk} |1_j 1_k\rangle. \quad (3.23)$$

Here N denotes the number of modes, $|2_j\rangle$ represents state with two photons in j th mode and vacuum in all other modes and $|1_j 1_k\rangle$ indicates state with one photon in modes j and k and no photons in the other modes.

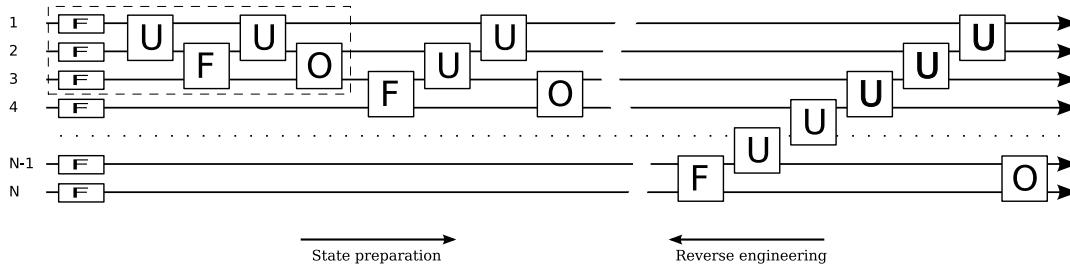


Figure 3.7: Scheme for preparation of generic N -mode two-photon state. As explained in the text, the scheme works in cycles. The scheme is composed of unitary transformations U that consist of a beam splitter and two phase shifters before and after the beam splitter, filters F equivalent to filter $F2$ from the scheme in Fig. 3.3, and the optimizing beam splitters O .

We begin by employing non-degenerate spontaneous parametric down-conversion to pro-

duce correlated state of two photons in $d = N/2$ pairs of modes ja and jb ,

$$|\psi_{\text{SPDC}}\rangle = \frac{1}{\sqrt{d}} \sum_{j=1}^d |1_{ja}\rangle |1_{jb}\rangle. \quad (3.24)$$

The modes ja and jb can be for instance different directions on the cone of the emission from the crystal [87]. Alternatively, one can pump the non-linear crystal with a sequence of d ultra-short pulses and then the modes ja and jb correspond to j th time-bin [88]. Yet another option is to simultaneously pump d nonlinear crystals. After down-conversion, the pairs of modes ja and jb are combined on d balanced beam splitters and the Hong-Ou-Mandel interference produces the state

$$|\psi_{\text{in}}\rangle = \frac{1}{\sqrt{N}} \sum_{j=1}^N |2_j\rangle. \quad (3.25)$$

In the second part of the protocol, the N -mode two-photon state (3.25) is injected into the interferometer shown in Fig. 3.7. The parameters of the interferometer can be again determined by reverse engineering where we let the target state propagate backwards through the scheme and at each step we eliminate certain component of the state by destructive interference. In this way we finally obtain the state (3.25). We now describe the cycles of the protocol in more detail. In the first cycle, we get rid of all states with exactly one photon in the last mode. First we apply unitary transformation to the first and second mode. This transformation is equivalent to the transformation U101 from Fig. 3.3 and eliminates the term $|100\dots001\rangle$. Next the second unitary transformation acting on the second and third mode eliminates the term $|010\dots001\rangle$. We continue in this fashion with only one exception. We do not use unitary transformation to mix the $(N-1)$ th and N th mode. Instead, we need to use a filter F similar to the filter F2 shown in Fig. 3.3, accompanied by attenuation of the first $N - 2$ modes (not shown in the figure). This filter removes the term $|00\dots11\rangle$. At this stage, all terms with exactly one photon in the last (N th) mode are eliminated and there is either zero or two photons in the last mode. For subsequent considerations it can be therefore neglected and we have effectively reduced the N -mode problem to $(N-1)$ -mode problem.

In the second cycle we apply the same strategy to eliminate all cross terms with one photon in the mode $N - 1$. Repeating this procedure $N - 3$ times we finally get back to the three-mode situation which we have already solved. The success probability of the protocol can be improved by employing optimizing beam splitters before each cycle. These beam

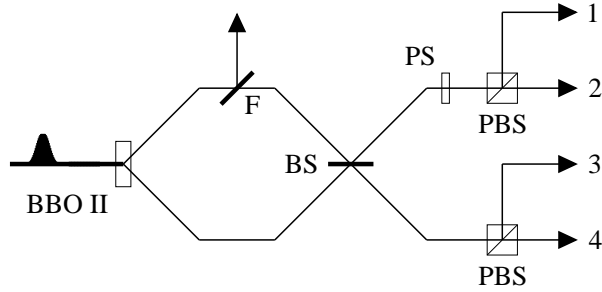


Figure 3.8: Scheme for preparation of the two-photon four-mode KLM states.

splitters play the same role as BS3 in Fig. 3.3 and they should combine the modes where the filter will be applied in a given cycle. The number of required two-mode operations that have to be implemented scales as $\frac{1}{2}N(N-1)$ with N being the number of modes.

3.6 Preparation of two-photon KLM states

The general scheme presented in the previous section can prepare any two-photon quantum state in an arbitrary number of modes. The experimental difficulty however increases considerably as the number of modes grows. If one is interested in preparation of specific class of quantum states then one could attempt to design a less general but simpler and experimentally more feasible scheme for this purpose. As an example of an important specific class of states we consider here the so-called two-photon four-mode KLM states,

$$|\psi_{\text{KLM}}\rangle = \alpha|1100\rangle + \beta|0110\rangle + \alpha|0011\rangle. \quad (3.26)$$

These states were introduced by Knill, Laflamme, and Milburn in the context of quantum computing with linear optics [11]. They can be used for teleportation-based implementation of quantum gates and the teleportation fidelity can be optimized by appropriate tuning of α/β ratio [12]. In view of these applications it is clearly important to be able to prepare such states in the simplest possible way.

The scheme for preparation of the two-photon KLM states is shown in Fig. 3.8. A strong coherent laser beam pumps nonlinear crystal BBO cut for Type-II phase matching where a maximally entangled two-photon triplet state $|\psi\rangle = \frac{1}{\sqrt{2}}(|H_1V_2\rangle + |V_1H_2\rangle)$ is generated in

the process of spontaneous parametric down-conversion (indexes 1 and 2 denote the spatial modes). The first spatial mode is then subjected to polarization sensitive filtering using a beam splitter F which entirely transmits vertical polarization and has amplitude transmissivity τ for horizontal polarization. In practice, such filtering can be accomplished, e.g., by means of tilted glass plates [89]. The two spatial modes are then combined on an ordinary (polarization in-sensitive) unbalanced beam splitter BS. We parametrize the transmittance t and reflectance r of BS by an angle ϑ and we have $t = \cos \vartheta$ and $r = \sin \vartheta$. In order to generate the desired state (3.26) we have to set

$$\vartheta = \arctan \sqrt{\tau}. \quad (3.27)$$

The polarization sensitive phase shifter PS adds a phase shift of π to the vertically polarized photon in the first output spatial mode. As a result of this entire procedure we obtain the state

$$|\psi\rangle = \alpha|H_1V_1\rangle + \beta|H_1V_2\rangle + \alpha|H_2V_2\rangle, \quad (3.28)$$

which can easily be split by two polarizing beam splitters to obtain the state (3.26) with parameters

$$\alpha = \sqrt{\frac{\tau}{1+\tau^2}}, \quad \beta = \frac{1-\tau}{\sqrt{1+\tau^2}}.$$

Since the scheme contains a filter F the state is prepared only probabilistically and the success probability is equal to $P_S = \frac{1}{2}(1 + \tau^2)$. Figure 3.9 illustrates the trade-off between success probability of the whole protocol and the probability $|\beta|^2$ of finding $|0110\rangle$ in the generated state. The teleportation protocol proposed by KLM requires the state (3.26) with $\alpha = \beta$ and for this case we find $P_S = 0.57$.

3.7 Conclusions

In this chapter we have demonstrated how entangled pairs of photons generated in the process of spontaneous parametric down-conversion can be used for preparation of an arbitrary multimode two-photon state. This preparation requires only linear optical elements (beam splitters, wave plates, phase shifters) whose parameters can be determined analytically by reverse engineering procedure whereby the target state is propagated backwards through the

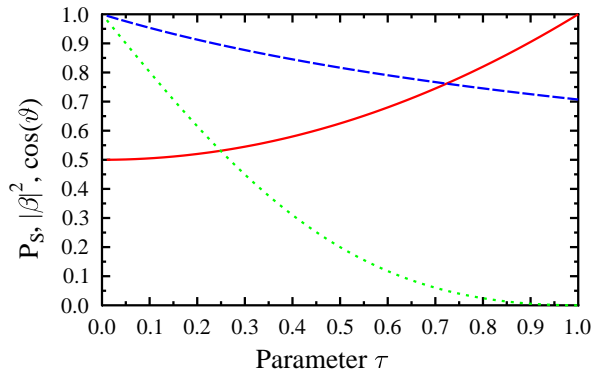


Figure 3.9: The success probability of the protocol (full red line), the probability of finding the state $|0110\rangle$ in the KLM state (dotted green line) and the amplitude transmissivity of the beam splitter BS (dashed blue line) are plotted as functions of the parameter τ .

scheme. We have also suggested a simple and experimentally feasible setup specifically tailored for preparation of two-photon KLM states which are crucial for linear optics quantum computing. The proposed schemes rely only on existing and well mastered experimental techniques and can be therefore implemented with current technology. Our findings thus pave the way towards generation of complex multimode entangled states of light required for advanced quantum information processing, ultraprecise measurements or quantum lithography.

Chapter 4

Preparation of entangled atomic Dicke states

4.1 Introduction

Quantum state of atomic ensemble can be described using collective atomic spin operators \hat{S}_x , \hat{S}_y and \hat{S}_z . By making the expectation value of one of these operators sufficiently large, the other two manifest similar algebraic properties as quadrature operators of light. One can use collective atomic spin operators to define the so-called Dicke states which are somewhat equivalent to Fock states of light. In this chapter, we propose a protocol for preparations of coherent superpositions of Dicke states of atoms. Such atomic quantum states can be expressed as

$$|\psi_{\text{target}}\rangle = \sum_{n=0}^N c_n |n\rangle, \quad (4.1)$$

where $|n\rangle$ denotes the n^{th} Dicke state. Our procedure is based on QND interaction between light and atoms and post-selection on outcomes of the measurement performed on output light beam. The general idea is to manipulate the atomic state by QND interaction with light, that has been previously prepared in a specific highly non-classical quantum state. This technique allows us to employ QND interaction to implement operations on atomic ensemble, that are not easy to perform directly on atoms, but are more feasible on light.

In the second section of this chapter, we will discuss the coupling of light and atoms, that

allows us to manipulate the atomic state. The third section shows how this coupling can be accompanied by atomic displacement operator implemented by application of magnetic field. The process of coupling and the usage of displacement operator are generalized to multiple interaction model in the section 4. We also present several numerical simulations in section 5.

4.2 Atoms-light interaction

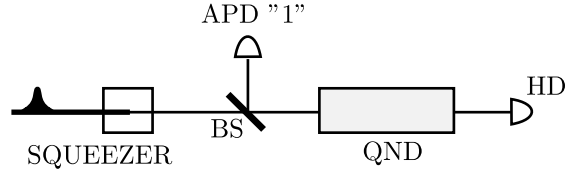


Figure 4.1: Atoms-light interaction setup. Light is prepared in squeezed vacuum state in the squeezer and then one photon is subtracted on the beam splitter BS. Light in such state accompanied by orthogonally polarized strong coherent beam interacts with atoms. After that, p_L quadrature measurement is performed on light using homodyne detection (HD).

Our proposal is based on setup schematically shown in figure 4.1. In this case, interaction between atoms and light can be described by Hamiltonian in the form of

$$\hat{H}_{QND} = \bar{\kappa} \hat{x}_L \hat{x}_A, \quad (4.2)$$

where \hat{x}_L denotes quadrature operator of light, \hat{x}_A quadrature operator of atoms and $\bar{\kappa}$ is the interaction constant. We suppose that atoms are in the initial state $|\phi_A\rangle$. As shown in figure 4.1, squeezed light beam is prepared in a squeezer pumped by a strong coherent laser beam. The beam then impinges on the beam splitter BS. We employ a highly unbalanced beam splitter with nearly unit transmissivity. Probability that two or more photons are reflected is then negligible. Click of the detector indicates one photon subtraction. This can be described by the action of annihilation operator on the state of the light beam

$$|\psi_L\rangle \longrightarrow \hat{a}|\psi_L\rangle. \quad (4.3)$$

The success probability of the whole procedure depends on the efficiency of the detector and also on the reflectivity of the beam splitter. One may increase the success probability

of the operation by using more reflective beam splitter. This will however result in higher probability of two photon reflection and therefore in lower fidelity of the prepared atomic state. Subsequently the QND interaction takes place followed by homodyne measurement (HD) of the \hat{p}_L quadrature operator of light, that is the conjugate light quadrature to \hat{x}_L quadrature appearing in (4.2). After the measurement, we post-select cases when the outcome is sufficiently close to zero. Description of the whole procedure can be written in mathematical terms as

$$\langle p_L = 0 | \exp\left(-i\hat{H}_{QND}t/\hbar\right)\hat{a}_L\hat{S}_L(r)|0_L\rangle|\phi_A\rangle, \quad (4.4)$$

where $\hat{S}_L(r) = \exp\left(\frac{-r}{2}\hat{a}_L^2 + \frac{r}{2}\hat{a}_L^{\dagger 2}\right)$ denotes the squeezing operator of light. Performing calculation of (4.4) we obtain the resulting operator

$$\hat{\Theta} = N\hat{x}_A \exp\left(-\kappa^2\hat{x}_A^2\right) \quad (4.5)$$

acting on atoms and describing their state manipulation. In (4.5) $\kappa = \frac{\bar{\kappa}t}{\hbar}e^r$ and N stands for normalization constant

$$N = \left(\frac{2}{\pi}\right)^{1/4} e^{-r/2} (e^{-2r} - 1) \frac{\kappa}{2}. \quad (4.6)$$

The operator $\hat{\Theta}$ is the key essence for Dicke states preparation. One can easily verify that action of $\hat{\Theta}$ on vacuum atomic state $|0_A\rangle$ leads to the final atomic state whose wave function reads

$$\langle x_A | \hat{\Theta} | 0_A \rangle = \left(\frac{2}{\pi}\right)^{1/4} N x \exp\left(-(\kappa^2 + 1)x^2\right) \quad (4.7)$$

and which is equivalent to the squeezed single-photon state (a.k.a. Schrödinger kitten-like state). By comparison with the wave function of $|1\rangle$ Dicke state, we notice, that the $\hat{\Theta}$ operator serves as creation and squeezing operator. This property can be exploited to generate superpositions of higher Dicke states.

4.3 Combination with displacement operator

Displacement operator $\hat{D}(\alpha)$ is one of several operators that are easily implemented on atomic ensemble by application of magnetic field resulting in a tiny rotation of the collective atomic spin. We propose to combine displacement operator and the $\hat{\Theta}$ operator. The entire operation

on atomic ensemble takes the form of

$$\hat{D}(\alpha_2)\hat{\Theta}\hat{D}(\alpha_1). \quad (4.8)$$

Calculation of the resulting state gives its wave function

$$\langle x_A | \hat{D}(\alpha_2)\hat{\Theta}\hat{D}(\alpha_1) | 0_A \rangle \propto (x - \Re\alpha_2) \exp \left[-(\kappa^2 + 1)x^2 + 2x(\Re\alpha_1 + (\kappa^2 + 1)\Re\alpha_2) + 2ix(\Im\alpha_1 + \Im\alpha_2) \right]. \quad (4.9)$$

Equation (4.9) resembles wave function of squeezed superposition of vacuum and $|1\rangle$ state. By changing the parameter α_2 , one can easily modify relative amplitudes of vacuum and $|1\rangle$ state as long as they remain real, without phase shift between these two states. The Gaussian part of the wave function has also to be centered on origin. This is accomplished simply by putting

$$\Im\alpha_1 = -\Im\alpha_2 \quad (4.10)$$

$$\Re\alpha_1 = -(\kappa^2 + 1)\Re\alpha_2, \quad (4.11)$$

which can be fulfilled without requiring more restrictions on superposition amplitudes.

4.4 Multiple interaction model

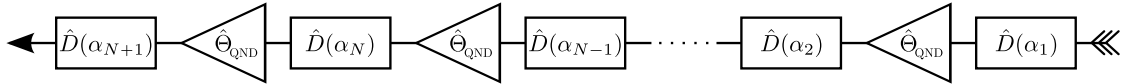


Figure 4.2: Schematized multiple interaction model as described by (4.12).

By repetition of (4.8) one is able to prepare superpositions of higher Dicke states. Such generalized operation reads as

$$\hat{D}(\alpha_{N+1})\hat{\Theta}\hat{D}(\alpha_N)\hat{\Theta}\hat{D}(\alpha_{N-1})\dots\hat{D}(\alpha_2)\hat{\Theta}\hat{D}(\alpha_1) \quad (4.12)$$

and is schematized in figure 4.2. Similar calculation as that leading to (4.7) gives us the general wave function as the result of the repeated action of displacement and theta operators.

Disregarding normalization constant this wave function can be divided into a set of products

$$A = \prod_{j=2}^{N+1} \left(x - \sum_{k=j}^{N+1} \Re\alpha_k \right) \quad (4.13)$$

$$B = \exp[-\kappa^2 N x^2] \quad (4.14)$$

$$C = \prod_{j=2}^{N+1} \exp \left(2\kappa^2 x \sum_{k=j}^{N+1} \Re\alpha_k \right) \quad (4.15)$$

$$D = \exp \left[- \left(x - \sum_{j=1}^{N+1} \Re\alpha_j \right)^2 \right] \quad (4.16)$$

$$E = \exp \left(2ix \sum_{j=1}^{N+1} \Im\alpha_j \right) \quad (4.17)$$

and thus written as

$$\psi(x) \propto ABCDE. \quad (4.18)$$

Inspired by (4.10), one can always set

$$\Im\alpha_1 = - \sum_{j=2}^{N+1} \Im\alpha_j \quad (4.19)$$

$$\Re\alpha_1 = - \sum_{j=2}^{N+1} \Re\alpha_j - \sum_{j=2}^{N+1} \sum_{k=j}^{N+1} \Re\alpha_k \quad (4.20)$$

and the Gaussian part of the wave function becomes centered on origin

$$\psi(x) \propto \prod_{j=2}^{N+1} \left(x - \sum_{k=j}^{N+1} \Re\alpha_k \right) \exp(-[\kappa^2 N + 1] x^2). \quad (4.21)$$

Wave function of any Dicke state is composed of product of a Hermite polynomial and a Gaussian function. Therefore also superpositions of Dicke states can be expressed as superpositions of these Hermite-Gauss functions. It is clear that the resulting wave function contains polynomial (A) with degree equal to the highest Dicke state in the target superposition and Gaussian part (B-E) containing also the parasitic squeezing induced by every QND interaction. The wave function of the target state (4.1) can be decomposed into a factorised form

$$\psi_{\text{target}}(x) = e^{-x^2} \sum_{n=0}^N c_n \frac{H_n(x)}{N_n} \propto e^{-x^2} \prod_{j=1}^{N+1} (x - R_j), \quad (4.22)$$

where $H_n(x)$ is the Hermite polynomial of the n^{th} degree and N_n is the normalization factor. By comparison with the wave function that results from multiple interaction model (4.21), we see that we are able to engineer the desired state just by setting correctly displacement parameters α_j . We need to find roots R_j of the polynomial and set

$$\begin{aligned}
\Re\alpha_{N+1} &= R_{N+1} \\
\Re\alpha_N &= R_N - \Re\alpha_{N+1} \\
\Re\alpha_{N-1} &= R_{N-1} - (\Re\alpha_{N+1} + \Re\alpha_N) \\
&\vdots \\
\Re\alpha_2 &= R_2 - \sum_{j=3}^{N+1} \Re\alpha_j.
\end{aligned} \tag{4.23}$$

Our protocol is capable of preparation of any superposition of Dicke states as long as all roots of the polynomial (4.13) remain real.

The resulting state differs from the pure superposition of Dicke states just by addition of $\kappa^2 N$ in the Gaussian function. This is the result of parasitic squeezing, which is affecting the wave function. To correct for this difference, we propose rescaling the calculated target state parameters

$$\alpha_j \longrightarrow \frac{\alpha_j}{\sqrt{\kappa^2 N + 1}}, \tag{4.24}$$

so that the state obtained by the procedure differs from the desired target state just by the squeezing in the x quadrature and can be described as $\hat{S}|\psi\rangle_{\text{target}}$. One may also employ an anti-squeezing operation that results in rescaling of quadrature operator

$$x \longrightarrow \frac{x}{\sqrt{\kappa^2 N + 1}} \tag{4.25}$$

and after such operation the obtained state will become the originally desired target state, that is the originally desired superposition of Dicke states.

4.5 Numerical simulations

Several numerical simulations have been carried out. These simulations verify the protocol functionality. As the result of our simulations, we have obtained Wigner functions of several target states (see fig. 4.3) [90]. For the purpose of these simulations, the interaction constant

has been set to $\kappa^2 = 0.2$. Our simulation program allows us not only to visualise the Wigner function of any target state, but calculates also correct parameters α_j for such state. If the state can not be obtained by this protocol due to complex root(s) in its polynomial, the program alerts us.

4.6 Conclusions

In this chapter, we have presented a protocol capable of preparation of a wide class of superpositions of Dicke states. The target state is limited only by the condition that all roots of its polynomial in the wave function must be real. We have also verified the proposed scheme by several numerical simulations. As for future plans, we are aimed to generalize our scheme to any superposition of Dicke states and analyse the success probability of our protocol in more detail.

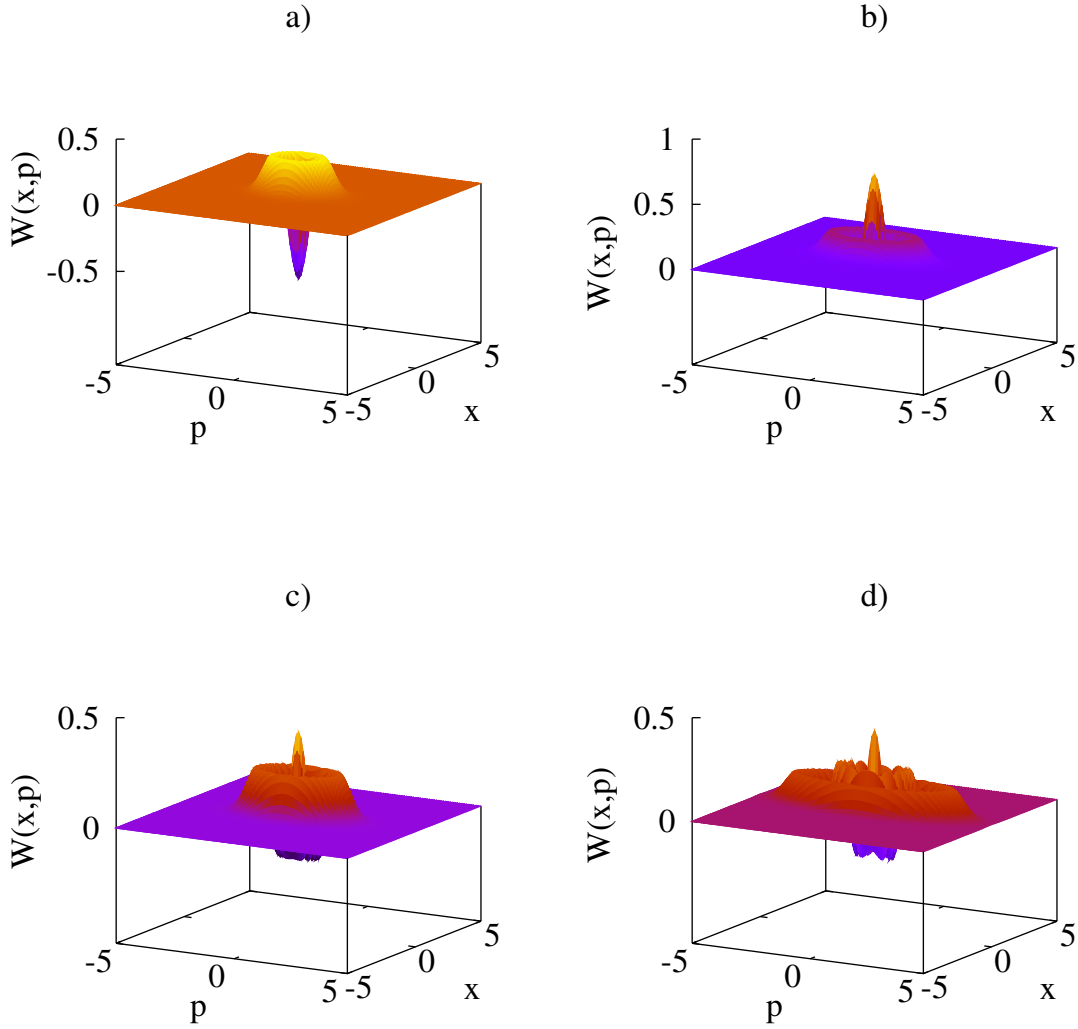


Figure 4.3: Wigner functions of several target states. Simulation has been performed using $\kappa^2 = 0.2$. a) $|1\rangle$, b) $\frac{1}{\sqrt{5}}(2|2\rangle + |0\rangle)$, c) $\frac{1}{\sqrt{3}}(|2\rangle + |1\rangle + |0\rangle)$, d) $\frac{1}{\sqrt{5}}(2|4\rangle + |1\rangle)$. One can observe the additional squeezing imposed on prepared states by the action of the $\hat{\Theta}$ operator.

Chapter 5

Conclusions

The field of interest of the present thesis is the generation of entangled quantum states of light and atoms. The work is divided into five chapters.

First chapter contains general introduction to the problematics and gets the reader familiar with already obtained results in the field of quantum states preparation.

Basic mathematics that is used throughout this thesis is presented to the reader in the second chapter. Quantum description of several optical devices, methods of light detection and interaction of light with atoms are treated in this chapter as well.

Third chapter contains our results on the preparation of entangled two-photon states in several spatial modes. Firstly, there is a mathematical proof that it is not possible to construct a deterministic passive linear optical scheme for preparation of arbitrary two-photon entangled states in several spatial modes. We therefore propose and analyze a non-deterministic scheme for preparation of two-photon states in three spatial modes. We discuss in detail the success probability of our scheme. Numerical simulations on two single-parametric classes of quantum states are also presented to the reader. These two simulations are accompanied by a histogram which shows that the average success probability of our scheme is about 26%. Generalization of the scheme to an arbitrary number of spatial modes is subsequently presented in this chapter. Proposed schemes are however experimentally rather challenging. For this reason, we have also proposed a less general scheme for preparation of two-photon KLM states. This scheme is limited to preparation of these specific states, but it is experimentally less demanding. The author would like to perform experimental demonstration of this scheme as

his future research. All schemes presented in this chapter use only linear optical elements and single photon detectors to verify successful preparation. Results of this research have already been published in a scientific journal [83].

The next, fourth, chapter presents our work in the area of preparation of Dicke states of atoms. We have proposed a scheme for preparation of superpositions of Dicke states. The scheme exploits the possibility of manipulation with atoms using a specifically prepared light beam. In combination with a magnetic field, which gives us the capability of implementing the displacement operator, we are able to prepare numerous superpositions of atomic Dicke states. In the scheme, we propose using squeezed light, single photon detector, homodyne detection and QND interaction between light and atoms. The work is accompanied by a numerical simulation yielding several Wigner functions of atomic states that can be prepared using our scheme.

This research was supported by the Ministry of Education of the Czech Republic under the project Centre of Modern Optics (LC06007).

Abstrakt diplomové práce

Diplomová práce se zabývá přípravou kvantově provázaných stavů světla a atomů a jejich možným využitím. Práce je rozdělena celkem do pěti kapitol a je sepsána v anglickém jazyce.

První kapitola se zabývá obecným úvodem do problematiky a seznamuje čtenáře s již dosaženými výsledky na poli přípravy kvantových stavů.

Druhá kapitola předkládá čtenáři základní matematický aparát, který byl využit při výzkumu. Zmíněn je kvantový popis několika optických komponent, způsobů detekce světla a také interakce světla s atomy.

Třetí kapitola obsahuje dosažené výsledky v přípravě kvantově provázaných stavů světla dvou fotonů v obecném počtu prostorových módů. Nejprve je proveden matematický důkaz, že v principu není možné sestavit schéma, které by dvoufotonové stavy v obecném počtu prostorových módů připravovalo deterministicky s využitím pouze pasivní lineární optiky. V práci je tedy předloženo a analyzováno nedeterministické schéma pro přípravu dvoufotonových stavů ve třech prostorových módech. Podrobně je diskutována úspěšnost schématu pro přípravu stavů světla a čtenáři jsou předloženy výsledky numerických simulací na dvou zvolených jednoparametrických třídách stavů. Pro lepší dokreslení byl rovněž vyhotoven histogram ukazující, že průměrná úspěšnost přípravy se pohybuje kolem 26%. Dále je zmíněné schéma zobecněno na libovolný počet prostorových módů a je tak získána zcela obecná metoda pro přípravu dvoufotonových stavů světla. Navržené postupy však jsou experimentálně obtížně realizovatelné, a proto je také předloženo schéma třetí, jehož cílem je příprava tzv. dvoufotonových KLM stavů. Toto schéma je schopné připravovat pouze zmíněné KLM stavy, je však experimentálně zvládnutelné a jeho realizací se bude autor zabývat při svém dalším studiu. Všechna schémata navrhovaná v této kapitole využívají pouze lineární optické komponenty a jednofotonové detektory pro ověření úspěchu přípravy. Výsledky výzkumu popisují

vaného v této kapitole byly publikovány v odborném časopise [83].

Následující, čtvrtá, kapitola popisuje výzkum v oblasti přípravy superpozice Dickeho stavů na atomech. Bylo navrženo schéma pro přípravu superpozicí Dickeho stavů. Schéma představuje možnost využití vhodným způsobem upraveného stavu světla k manipulaci s atomy. V kombinaci s magnetickým polem, kterým realizujeme operátor posunutí, lze připravit celou řadu Dickeho stavů a jejich superpozice. Schéma počítá s využitím zdroje stlačeného světla, jednofotonového detektoru, homodynní detekce a QND interakce světla s atomy. Jako výsledek přípravy je prezentována numerická simulace znázorňující Wignerovy funkce několika zvolených atomových stavů, které je možné pomocí navrženého schémata připravit.

Poslední kapitola diplomové práce stručně shrnuje dosažené výsledky a předkládá další plány do budoucna.

Výzkum popsáný v této diplomové práci byl podporován Ministerstvem školství, mládeže a tělovýchovy České republiky v rámci projektu Centrum moderní optiky (LC06007).

Résumé de la thèse

Cette thèse est consacrée à la préparation de états quantiques intriqués de la lumière et des atomes. Le travail est divisé en cinq chapitres et il est écrit en langue anglaise.

Le premier chapitre donne au lecteur des informations générales sur la problématique et fait un résumé des résultats déjà obtenus en ce qui concerne la préparation des états quantiques.

Le deuxième chapitre énonce le traitement mathématique comme il est ensuite utilisé dans le reste de la thèse. La description de quelques outillages d'optique, des méthodes de détection de la lumière et de l'interaction de la lumière avec des atomes est aussi présentée dans ce chapitre.

Le troisième chapitre contient des proposition des schémas qui permettent de préparer des états quantiques de deux photons dans le nombre de modes arbitraire. Premièrement, on a bien démontré que la construction d'un schéma qui prépare ces état de la manière déterministe est impossible en n'utilisant que l'optique linéaire passive. On a alors proposé et analysé un schéma non-déterministe pour préparer des états quantiques de deux photons dans trois modes. On discute aussi en détail la probabilité de succès de notre schéma. Pour une meilleure illustration, on a ajouté un histogramme qui montre que la probabilité de succès moyenne est de 26%. Le schéma est successivement généralisé au nombre de modes arbitraire. Les propositions nécessitent malheureusement un effort considérable pour les réaliser expérimentalement. C'est pourquoi, on a aussi proposé un schéma capable de préparer les état KLM de deux photons. Ce schéma est limité à la classe de ces états spécifiques, mais il peut être réalisé expérimentalement. Cette réalisation est un des objectifs futures de l'auteur. Tous les schémas présentés dans ce chapitre n'utilise que des outillages d'optique linéaires et des détecteurs de photons singuliers pour la vérification de préparation. Les résultats décrits

dans ce chapitre étaient publiés dans un journal scientifique [83].

Le quatrième chapitre décrit notre recherche dans le domaine de préparation des superpositions des états de Dicke des atomes. On a proposé un schéma de préparation de ces états. Le schéma représente la possibilité d'utiliser l'interaction des atomes avec de la lumière préparée dans un état spécifique pour manipuler l'état atomique. En utilisant cette interaction accompagnée par l'application du champ magnétique qui permet d'effectuer l'opération de déplacement, on est capable de préparer une classe étendue des superpositions des états de Dicke. Le schéma contient le générateur de la lumière comprimée, un détecteur de photons, une détection homodyne et l'interaction non-destructive de la lumière avec des atomes. Les résultats de préparation des états sont présentés sous la forme d'une simulation numérique qui montre quelques fonctions de Wigner des états qui peuvent être préparés par notre schéma.

Le dernier chapitre fait une conclusion de la thèse et énonce aussi quelques plans pour le future.

La recherche décrite dans cette thèse de mastère était supportée par le Ministère de l'éducation de la République Tchèque sous le projet Centre de l'optique moderne (LC06007).

Bibliography

- [1] M. Planck: *Annalen der Physik* **1** (1900) 719
- [2] Wikipedia: *Quantum optics* — *wikipedia, the free encyclopedia* (2008): [Online; accessed 10-April-2008]
- [3] Wikipedia: *Laser* — *wikipedia, the free encyclopedia* (2008): [Online; accessed 10-April-2008]
- [4] G. Alber, T. Beth, M. Horodecki: *Quantum Information*: Springer, Berlin (2001)
- [5] D. Boumeester, A. Ekert, A. Zeilinger: *The Physics of Quantum Information*: Springer, Berlin (2000)
- [6] M. Nielsen, I. Chuang: *Quantum Computation and Quantum Information*: Cambridge University Press, Cambridge (2002)
- [7] C. Bennett, G. Brassard, C. Crépeau, R. Jozsa, A. Peres, W. Wothers: *Phys. Rev. Lett.* **70** (1993) 1895
- [8] D. Bouwmeester, J. Pan, K. Mattle, M. Eibl, H. Weinfurter, A. Zeilinger: *Nature (London)* **390** (1997) 575
- [9] S. Braunstein, H. Kimble: *Phys. Rev. Lett.* **80** (1998) 869
- [10] A. Furusawa, J. Sorensen, S. Braunstein, C. Fuchs, H. Kimble, E. Polzik: *Science* **282** (1998) 706
- [11] E. Knill, R. Laflamme, G. Milburn: *Nature (London)* **409** (2001) 46

- [12] J. Franson, M. Donegan, M. Fitch, B. Jacobs, T. Pittman: *Phys. Rev. Lett.* **89** (2002) 137901
- [13] T. Pittman, B. Jacobs, J. Franson: *Phys. Rev. A* **71** (2005) 032307
- [14] N. Kiesel, C. Schmid, U. Weber, R. Ursin, H. Weinfurter: *Phys. Rev. Lett.* **95** (2005) 210505
- [15] S. Gasparoni, J. Pan, P. Walther, T. Rudolph, A. Zeilinger: *Phys. Rev. Lett.* **93** (2004) 020504
- [16] J. O'Brien, G. Pryde, A. White, T. Ralph, D. Branning: *Nature (London)* **426** (2003) 264
- [17] T. Pittman, B. Jacobs, J. Franson: *Phys. Rev. A* **64** (2001) 062311
- [18] H.-J. Briegel, W. Dür, J. I. Cirac, P. Zoller: *Phys. Rev. Lett.* **81** (1998) 5932
- [19] A. I. Lvovsky, H. Hansen, T. Aichele, O. Benson, J. Mlynek, S. Schiller: *Phys. Rev. Lett.* **87** (2001) 050402
- [20] A. Zavatta, S. Viciani, M. Bellini: *Phys. Rev. A* **70** (2004) 053821
- [21] A. Ourjoumtsev, R. Tualle-Brouiri, P. Grangier: *Phys. Rev. Lett.* **96** (2006) 213601
- [22] A. E. B. Nielsen, K. Molmer: *Phys. Rev. A* **75** (2007) 043801
- [23] M. Dakna, T. Anhut, T. Opatrný, L. Knöll, D.-G. Welsch: *Phys. Rev. A* **55** (1997) 3184
- [24] A. Ourjoumtsev, R. Tualle-Brouiri, J. Laurat, P. Grangier: *Science* **312** (2006) 83
- [25] J. S. Neergaard-Nielsen, B. M. Nielsen, C. Hettich, K. M. Imer, E. S. Polzik: *Phys. Rev. Lett.* **97** (2006) 083604
- [26] K. Wakui, H. Takahashi, A. Furusawa, M. Sasaki: *Opt. Express* **15** (2007) 3568
- [27] A. Ourjoumtsev, H. Jeong, R. Tualle-Brouiri, P. Grangier: *Nature (London)* **448** (2007) 784
- [28] A. Zavatta, S. Viciani, M. Bellini: *Science* **306** (2004) 660

- [29] M. Dakna, J. Clausen, L. Knöll, D.-G. Welsch: *Phys. Rev. A* **59** (1999) 1658
- [30] J. Fiurášek, R. García-Patrón, N. J. Cerf: *Phys. Rev. A* **72** (2005) 033822
- [31] J. Fiurášek, S. Massar, N. J. Cerf: *Phys. Rev. A* **68** (2003) 042325
- [32] M. Mitchell, J. Lundeen, A. Steinberg: *Nature (London)* **429** (2004) 161
- [33] P. Kok, H. Lee, J. Dowling: *Phys. Rev. A* **65** (2002) 052104
- [34] J. Fiurášek: *Phys. Rev. A* **65** (2002) 053818
- [35] H. Lee, P. Kok, N. Cerf, J. Dowling: *Phys. Rev. A* **65** (2002) 030101
- [36] H. Hofmann: *Phys. Rev. A* **70** (2004) 023812
- [37] A. E. B. Nielsen, K. Molmer: *Phys. Rev. A* **75** (2007) 063803
- [38] H. Cable, J. P. Dowling: *Phys. Rev. Lett.* **99** (2007) 163604
- [39] K. T. Kapale, J. P. Dowling: *Phys. Rev. Lett.* **99** (2007) 053602
- [40] F. W. Sun, Z. Y. Ou, G. C. Guo: *Phys. Rev. A* **73** (2006) 023808
- [41] B. Yurke: *Phys. Rev. Lett.* **56** (1986) 1515
- [42] M. Hillery, L. Mlodinow: *Phys. Rev. A* **48** (1993) 1548
- [43] C. Brif, A. Mann: *Phys. Rev. A* **54** (1996) 4505
- [44] J. Dowling: *Phys. Rev. A* **57** (1998) 4736
- [45] K. J. Resch, K. L. Pagnell, R. Prevedel, A. Gilchrist, G. J. Pryde, J. L. O'Brien, A. G. White: *Phys. Rev. Lett.* **98** (2007) 223601
- [46] A. Boto, P. Kok, D. Abrams, S. Braunstein, C. Williams, J. Dowling: *Phys. Rev. Lett.* **85** (2000) 2733
- [47] G. Bjork, L. Sanchez-Soto, J. Soderholm: *Phys. Rev. Lett.* **86** (2000) 4516
- [48] M. D'Angelo, M. Chekhova, Y. Shih: *Phys. Rev. Lett.* **87** (2001) 013602

- [49] A. E. Kozhokin, K. Mølmer, E. Polzik: *Phys. Rev. A* **62** (2000) 033809
- [50] K. Surmacz, J. Nunn, F. C. Waldermann, Z. Wang, I. A. Walmsley, D. Jaksch: *Phys. Rev. A* **74** (2006) 050302
- [51] C. Mewes, M. Fleischhauer: *Phys. Rev. A* **72** (2005) 022327
- [52] A. Dantan, J. Cviklinski, M. Pinard, P. Grangier: *Phys. Rev. A* **73** (2006) 032338
- [53] T. Opatrny: *Phys. Rev. A* **74** (2006) 043809
- [54] B. Julsgaard, J. Sherson, J. I. Cirac, J. Fiurasek, E. S. Polzik: *Nature (London)* **432** (2004) 482
- [55] D. N. Matsukevich, A. Kuzmich: *Science* **306** (2004) 663
- [56] T. Opatrny, J. Fiurasek: *Phys. Rev. Lett.* **95** (2005) 053602
- [57] V. Bužek, H. Moya-Cessa, P. L. Knight, S. J. D. Phoenix: *Phys. Rev. A* **45** (1992) 8190
- [58] J. Fiurasek, J. Sherson, T. Opatrny, E. S. Polzik: *Phys. Rev. A* **73** (2006) 022331
- [59] A. Dantan, A. Bramati, M. Pinard: *Phys. Rev. A* **71** (2005) 043801
- [60] J. I. Cirac, P. Zoller, H. J. Kimble, H. Mabuchi: *Phys. Rev. Lett.* **78** (1997) 3221
- [61] X. Maître, E. Hagley, G. Nogues, C. Wunderlich, P. Goy, M. Brune, J. M. Raimond, S. Haroche: *Phys. Rev. Lett.* **79** (1997) 769
- [62] H. Jing, X.-J. Liu, M.-L. Ge, M.-S. Zhan: *Phys. Rev. A* **71** (2005) 062336
- [63] J. Nunn, I. A. Walmsley, M. G. Raymer, K. Surmacz, F. C. Waldermann, Z. Wang, D. Jaksch: *Phys. Rev. A* **75** (2007) 011401
- [64] D. R. Sypher, I. M. Breerton, H. M. Wiseman, B. L. Hollis, B. C. Travaglione: *Phys. Rev. A* **66** (2002) 012306
- [65] H.-J. Briegel, W. Dür, J. I. Cirac, P. Zoller: *Phys. Rev. Lett.* **81** (1998) 5932
- [66] L. M. Duan, M. D. Lukin, J. I. Cirac, P. Zoller: *Nature (London)* **414** (2001) 413

- [67] A. Kuzmich, E. S. Polzik: *Phys. Rev. Lett.* **85** (2000) 5639
- [68] W. Rosenfeld, S. Berner, J. Volz, M. Weber, H. Weinfurter: *Phys. Rev. Lett.* **98** (2007) 050504
- [69] M. Brune, S. Haroche, J. M. Raimond, L. Davidovich, N. Zagury: *Phys. Rev. A* **45** (1992) 5193
- [70] C. Schori, B. Julsgaard, J. L. Sørensen, E. S. Polzik: *Phys. Rev. Lett.* **89** (2002) 057903
- [71] G. S. Agarwal, R. R. Puri, R. P. Singh: *Phys. Rev. A* **56** (1997) 2249
- [72] C. C. Gerry, R. Grobe: *Phys. Rev. A* **56** (1997) 2390
- [73] C. C. Gerry, R. Grobe: *Phys. Rev. A* **57** (1998) 2247
- [74] S. Chen, Y.-A. Chen, B. Zhao, Z.-S. Yuan, J. Schmiedmayer, J.-W. Pan: *Phys. Rev. Lett.* **99** (2007) 180505
- [75] M. D. Lukin, S. F. Yelin, M. Fleischhauer: *Phys. Rev. Lett.* **84** (2000) 4232
- [76] A. Dantan, G. Reinaudi, A. Sinatra, F. Laloe, E. Giacobino, M. Pinard: *Phys. Rev. Lett.* **95** (2005) 123002
- [77] C. Langer, R. Ozeri, J. D. Jost, J. Chiaverini, B. DeMarco, A. Ben-Kish, R. B. Blakestad, J. Britton, D. B. Hume, W. M. Itano, D. Leibfried, R. Reichle, T. Rosenband, T. Schaetz, P. O. Schmidt, D. J. Wineland: *Phys. Rev. Lett.* **95** (2005) 060502
- [78] W. Greiner, B. Muller: *Quantum Mechanics*: Springer, Berlin (1989)
- [79] J. Perina: *Quantum Statistics of Linear and Nonlinear Optical Phenomena*: Informatorium, 2nd edn. (1991)
- [80] S. L. Braunstein, P. van Loock: *Reviews of Modern Physics* **77** (2005) 513
- [81] J. J. Sakurai: *Modern Quantum Mechanics*: Addison-Wesley Publishing Company, Inc., revised edn. (1994)
- [82] C. Hong, Z. Ou, L. Mandel: *Phys. Rev. Lett.* **58** (1987) 2044

- [83] K. Lemr, J. Fiurasek: *Phys. Rev. A* **77** (2008) 023802
- [84] N. M. VanMeter, P. Lougovski, D. B. Uskov, K. Kieling, J. Eisert, J. P. Dowling: *Phys. Rev. A* **76** (2007) 063808
- [85] M. Paris, J. Řeháček: *Quantum State Estimation*: Springer, Berlin (2004)
- [86] M. Reck, A. Zeilinger: *Phys. Rev. Lett.* **73** (1994) 58
- [87] C. Cinelli, M. Barbieri, R. Perris, P. Mataloni, F. D. Martini: *Phys. Rev. Lett.* **95** (2005) 240405
- [88] D. Stucki, H. Zbinden, N. Gisin: *Journal of Modern Optics* **52** (2005) 2637
- [89] A. Cernoch, L. Bartuskova, J. Soubusta, M. Jezek, J. Fiurasek, M. Dusek: *Phys. Rev. A* **74** (2006) 042327
- [90] A. Kenfack, K. Zyczkowski: *Journal of Optics B* **6** (2004) 396